Article

The Structure-Activity Relationships of Spectinamide Antituberculosis agents; a Dissection of Ribosomal Inhibition and Native Efflux Avoidance Contributions

Jiuyu Liu, David F. Bruhn, Robin B. Lee, Zhong Zheng, Tanja Janusic, Dimitri Scherbakov, Michael S. Scherman, Helena I.M. Boshoff, Sourav Das, * Raskesh, Samanthi L. Waidyarachchi, Tiffany A. Brewer, Begona Gracia, Lei Yang, John C. Bollinger, Gregory T. Robertson, Bernd Meibohm, Anne J. Lenaerts, Jose Ainsa, Erik C. Böttger, and Richard E Lee

Just Accepted

The Structure-Activity Relationships of Spectinamide Antituberculosis agents; a Dissection of Ribosomal Inhibition and Native Efflux Avoidance Contributions

Jiuyu Liu,[1] David F. Bruhn,[1] Robin. B. Lee,[1] Zhong Zheng,[1] Tanja Janusic,[2] Dimitri Scherbakov,[2] Michael S. Scherman,[3] Helena I. Boshoff,[4] Sourav Das,[1] Rakesh,[1] Samanthi L. Waidyarachchi,[1] Tiffany A. Brewer, [1,5] Begoña Gracia,[6] Lei Yang,[1] John Bollinger,[1] Gregory T. Robertson,[3] Bernd Meibohm,[5] Anne J. Lenaerts,[3] Jose Ainsa,[6] Erik C. Böttger,[2] Richard E. Lee[1*]

1. Department of Chemical Biology and Therapeutics, St. Jude Children's Research Hospital, 262 Danny Thomas Place, MS#1000, Memphis, Tennessee, 38105, USA

2. Institut für Medizinische Mikrobiologie, Nationales Zentrum für Mykobakterien, Universität Zürich, Rämistrasse 71, Gloriastrasse 30/32, CH-8006 Zürich, Switzerland

3. Mycobacterial Research Laboratories, Department of Microbiology, Colorado State University, 1682 Campus Delivery, Fort Collins, Colorado, 80523, USA

4. Tuberculosis Research Section, Laboratory of Clinical Infectious Diseases, National Institute for Allergy and Infectious Disease, National Institutes of Health, 33 North drive, Bethesda, Maryland, 20814, USA

5. Department of Pharmaceutical Sciences, University of Tennessee Health Science Center, 881 Madison Avenue, Memphis, TN 38163, USA

6. Departamento de Microbiología, Medicina Preventiva y Salud Pública, and BIFI, Universidad de Zaragoza, 50009-Zaragoza, and CIBER Enfermedades Respiratorias (CIBERES), Spain

Correspondence should be addressed to R.E.L. (Richard.Lee@StJude.org)

ABSTRACT

Spectinamides are a novel class of antitubercular agents with the potential to treat drug resistant tuberculosis infections. Their antitubercular activity is derived from both ribosomal affinity and their ability to overcome intrinsic efflux mediated by the *Mycobacterium tuberculosis* Rv1258c efflux pump. In this study we explore the structure activity relationships through analysis of 50 targeted spectinamides. Compounds are evaluated for ribosomal translational inhibition, MIC activity in Rv1258c efflux pump deficient and wild type tuberculosis strains, and efficacy in an acute model of tuberculosis infection. The results of this study show a narrow structure-activity relationship, consistent with a tight ribosome binding pocket and strict structural requirements to overcome native efflux. Rationalization of ribosomal inhibition data using molecular dynamics simulations showed stable complex formation for halogenated spectinamides consistent with the long post antibiotic effects observed. The lead spectinamides identified in this study demonstrated potent MIC activity against MDR and XDR tuberculosis and had desirable antitubercular class specific features including: low protein binding, low microsomal metabolism, no cytotoxicity, and significant reductions in bacterial burdens in the lungs of mice infected with *M. tuberculosis*. The structure activity relationships detailed here emphasize the need to examine efflux-mediated resistance in the design of antituberculosis drugs and demonstrate that it is possible to overcome intrinsic efflux with synthetic modification. The ability to understand the structure requirements for this class has produced a variety of new substituted spectinamides, which may provide useful alternative candidates and promote the further development of this class.

1
2
3
4
5
6
7
8
9
10
11
12
13
14
15
16
17
18
19
20
21
22
23
24
25
26
27
28
29
30
31
32
33
34
35
36
37
38
39
40
41
42
43
44
45
46
47
48
49
50
51
52
53
54
55
56
57
58
59
60

KEYWORDS: Structure-Activity Relationship, spectinamide, spectinomycin, antituberculosis,

efflux pump, efficacy.

Introduction

Despite decades of chemotherapeutic intervention, tuberculosis infection remains a leading cause of death worldwide. The increasing incidence of drug resistant tuberculosis infections and reports of infections resistant to all available antibiotics highlight the striking and urgent need for new tuberculosis drugs and treatment regimes.[1-3] We have recently demonstrated that synthetic modification of spectinomycin is a robust approach to enhancing this potent ribosome inhibitor's antibacterial activity towards respiratory tract bacterial infections, including *Mycobacterium tuberculosis*.[4]

Spectinomycin is a natural product aminocyclitol produced by *Streptomyces spectabilis*. It is a bacterial ribosome inhibitor that binds selectively to a unique binding site in RNA helix 34 of the head domain of the bacterial 30S ribosomal subunit, blocking translocation and consequently protein synthesis.[5-6] Unfortunately, spectinomycin lacks antibacterial activity towards common bacterial pathogens primarily due to efflux mechanisms.[4, 7] It is, however, an attractive scaffold for the design of new agents since it is a potent inhibitor of bacterial ribosomes but not mammalian ribosomes, it has an established high safety profile, and unlike other aminoglycosides it does not have any reported ototoxicity or nephrotoxicity.[8] The structure of spectinomycin is unique amongst aminoglycoside antibiotics in which actinamine forms both acetal and hemiacetal linkages with actinospectose.[9] Previous efforts to develop spectinomycin analogs with improved whole cell potency in the 1980's indicated that the actinamine ring portion of spectinomycin could not be modified without compromising potency,[10-12] but modifications to the 3' and 5' positions of actinospectose ring (C-ring) were well tolerated.[13-15] Utilizing these early drug discovery studies and our modern knowledge of the molecular interaction of spectinomycin with the bacterial ribosome,[6] we have been able to generate two

chemically distinct series of spectinomycins: spectinamides with narrow spectrum activity

against *M. tuberculosis*;[4] and the aminomethyl spectinomycins active against a broader range of

respiratory tract and sexually transmitted bacterial pathogens.[16]

This report examines the detailed structure activity relationship (SAR) of our antitubercular

spectinamide series. The spectinamides lack cross-resistance with existing tuberculosis

therapeutics, retain spectinomycin's high selectivity index and are efficacious *in vivo* against

multiple mouse models of tuberculosis infection. Spectinomycin's weak activity in *M.*

tuberculosis is the result of efflux by Rv1258c. Unlike spectinomycin, lead spectinamides are

not subject to efflux by Rv1258c, which is particularly notable given the upregulation of this

pump in some strains of multiple drug resistance (MDR) tuberculosis and its role in macrophage

induced drug tolerance.[17] Herein, we report the synthesis of 41 new spectinamides and present a

comprehensive SAR study (50 analogs in total) for this series, discussing the structural

requirements for potent inhibition of bacterial protein synthesis, efflux avoidance, and

antituberculosis activity *in vitro* and *in vivo*.

Results and Discussion

Chemistry.

The spectinamides were synthesized in a rapid four-step protocol from spectinomycin using the

general procedure of Woitun (Scheme 1).[15] Structural diversity was incorporated into the

sidechain in the key acylation step using targeted aryl acids. Optimization of the final

deprotection step was performed by either catalytic hydrogenation, using palladium on carbon in

methanolic HCl for 2 h, or in the case of hydrogenation-sensitive side chains by acid hydrolysis

with 48% HBr solution at room temperature for 2 h. During scale up for *in vivo* testing, the

synthesis protocol for many compounds can be further simplified by crystallization of

carboxybenzyl (Cbz) protected intermediate after the key acylation step. This removes the need

for column chromatography. The spectinamides were provided as neutral dihydrochloride salts

for biological testing unless otherwise noted.
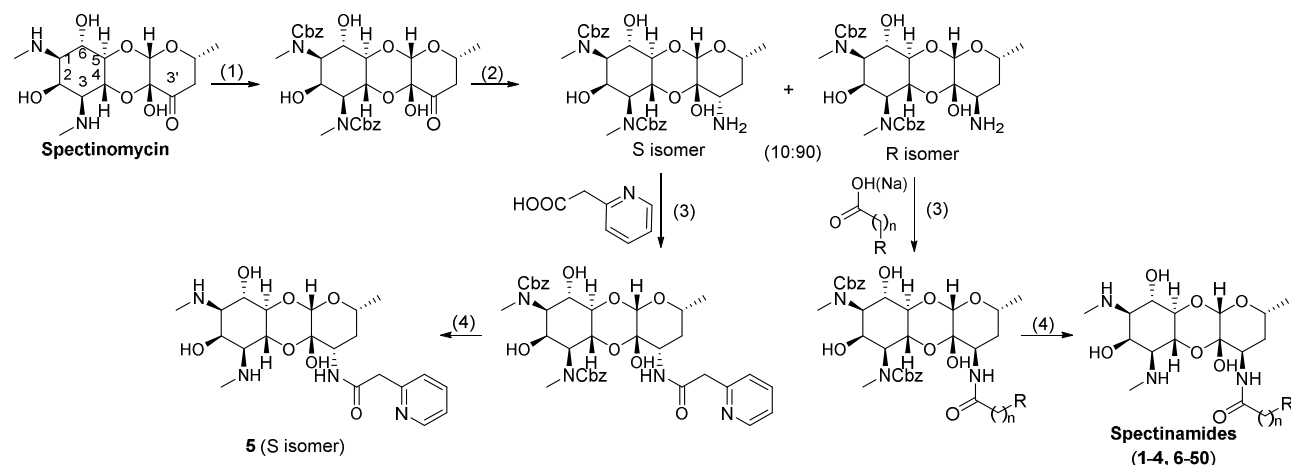
Scheme 1. Reagents and conditions: (1) BnOCOCl, NaHCO₃, acetone/water, room temperature,

10 h, 90%; (2) NH₄NO₃, 2-Methylpyridine borane , 10% acetic acid in methanol, room

temperature, 2 h, 40%; (3) HBTU, DIPEA, DMF, room temperature; (4) method 1, 10% Pd/C,

1M HCl in MeOH; method 2, 48% HBr.

To verify the stereochemistry of spectinamides, the tri-hydrobromide salt **1** (Figure 1A) was

crystalized from methanol-acetone and the resulting crystal structure was determined (Figure 1B,

Supplementary Table S1). These results confirmed the *R* stereochemistry assignment in the key

3' position amino substitution position of the actinospectose ring of the bioactive spectinamides.

To make the 3'-(S) isomer of **1**, the 3'-epimeric amine was isolated after the reductive amination

step as a minor component by chromatography. This enantiomer was then taken through the

same reaction scheme as **1** to generate the corresponding 3' epimer, **5.**
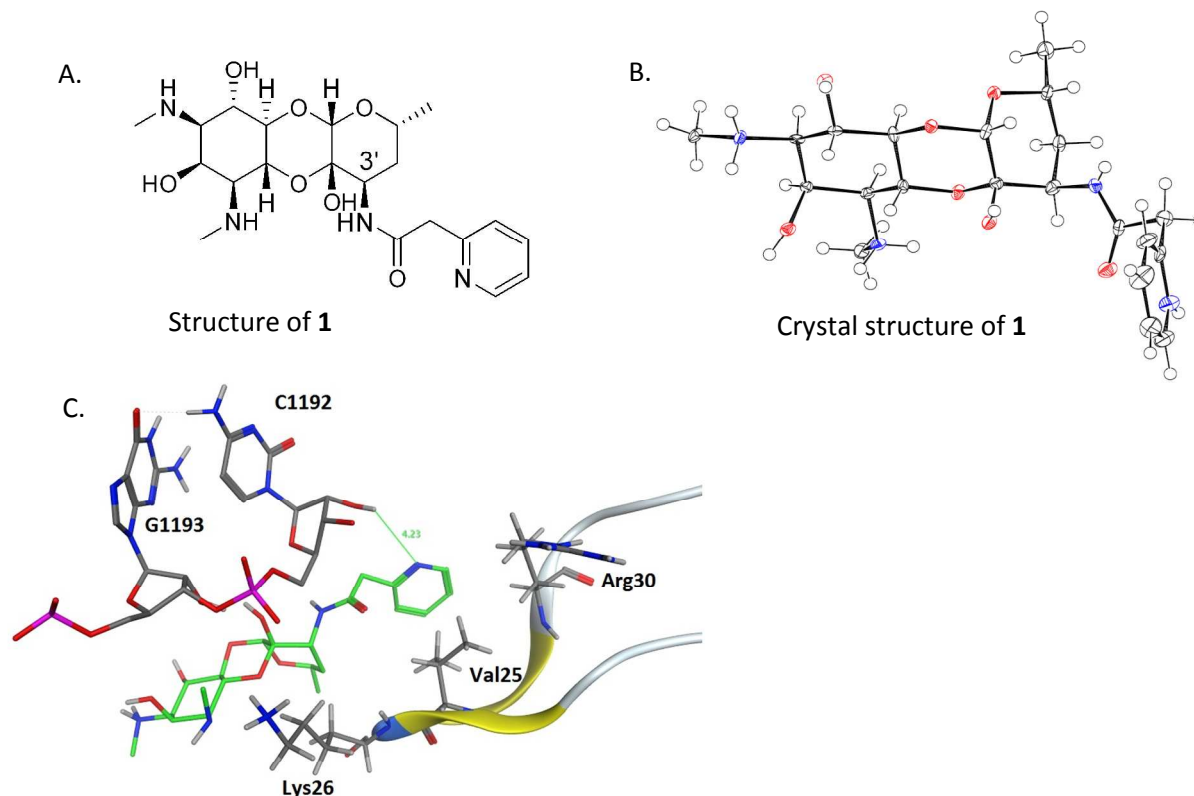
Figure 1: A. Structure of 1. B. Crystal structure of 1 that confirms 3' stereochemical assignment of bioactive spectinamides; C. Spectinamide 1 ribosomal binding mode modeled from a 20 ns molecular dynamics simulation. The nitrogen atom of the pyridine ring is shown to interact with the hydroxyl group of C1192. The spectinamide side chain binding pocket is formed between helix 31 and the RpsE interaction loop. Valine 25 of the RpsE loop is positioned to form a van der Waals' interaction with the pyridine ring.

Design and Prior SAR observations.

Computational modeling of 1 in the *M. tuberculosis* ribosome revealed an unexplored pocket adjacent to helix 31 and the RpsE loop that is accessed by the aryl spectinamide side chain (Figure 1C). This model indicated hydrogen bonding between the 2-pyridyl moiety of 1 to hydroxyl groups of C1192 and G1193 that held the ring in position in the pocket. Our original

panel of 16 spectinamide analogs included compound **2**, which only has a phenyl ring and lacks

the 2-pyridyl functionality, as well as compounds **3** and **4**, which have the 3- and 4-pyridyl,

respectively. These compounds were interesting as the ribosomal IC_{50}s were slightly increased

(3.02-5.07 µg/ml, Table 1), but the minimum inhibitory concentrations (MICs) for these

compounds were much higher (50-200 µg/ml, Table 1), more than could be expected based on

the less dramatic change in ribosomal inhibition. When this set of compounds was tested against

M. tuberculosis with Rv1258c inactivated, the MIC of compounds **2**, **3** and **4** decreased

substantially (16-32 fold), but the MIC of **1** remained the same (Table 1). This set of compounds

confirmed that the 2-pyridyl introduces favorable interactions with the ribosomal active site and

indicated it is necessary for avoidance of efflux by pump Rv1258c.

Based on our model of **1** bound to the active site, we proposed three series of modifications to

build the SAR of the series: exploration of the linker to incorporate a spacer that orients the

pyridyl ring in the ribosome side chain binding site; bioisosteric replacement of the 2-pyridyl

ring with different heteroaryl ring systems to enable increased structural diversity; introduction

of electron withdrawing (EW) or electron donating (ED) groups into the pyridine ring to explore

how altering the electrochemical properties of the ring affects ribosome binding and efflux.

Compounds were tested *in vitro* for inhibition of ribosomal translation using purified *M.*

smegmatis ribosomes, whole cell activity against *M. tuberculosis* H37Rv, and for activity against

the efflux deficient *M. tuberculosis* H37Rv Rv1258c knockout (KO). Compounds fell into four

categories: i) modifications that resulted in a loss of ribosomal activity; ii) modifications that

retained ribosomal inhibition and have similar whole cell activity against both H37Rv wild type

and the Rv1258c KO, indicating the modification enables the compound to avoid efflux; iii)

modifications that retained ribosomal inhibition, but have greater than 2 fold differences in

whole cell activity between H37Rv and the Rv1258c KO, indicating they are subject to efflux;

iv) modifications that retained ribosomal inhibition, but resulted in decrease in activity against

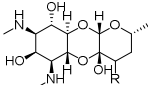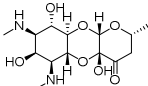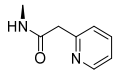H37Rv, indicating a possible reduction in cell permeability, uptake, or accumulation.
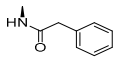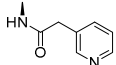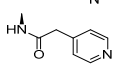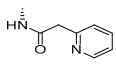
To examine the importance of the chirality of the 3' position at the spectinamide core, the 3'-(S)-

isomer of **1** was synthesized (compound **5**) and found to be inactive in both whole cell and

ribosomal assays (MIC >200 µg/ml, IC$_{50}$ 42.23 µg/ml). This confirmed the antitubercular

activity of **1** remains on target and its antimicrobial activity is dependent on ribosomal inhibition.
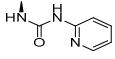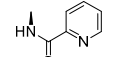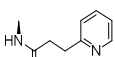
Modification to the linker.

Four linker derivatives were synthesized incorporating amine (**6**), carbamate (**7**), urea (**8**), and

sulfonamide (**9**) linkages. In these initial studies, the phenyl aromatic ring was utilized as 2-

pyridyl precursors were not commercially available. The lack of the 2-pyridyl resulted in MICs

of 200 µg/ml or greater, and this subset therefore did not contribute to the MIC SAR and were

only considered for ribosomal inhibition. Isosteric linker changes were generally not well

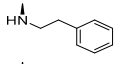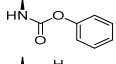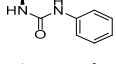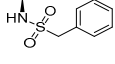tolerated with respect to ribosomal inhibition, only compound urea **8** (3.77 µg/ml) had

antiribosomal activity similar to **2** (3.02 µg/ml). This compound was later remade to include the

2-pyridyl ring in combination with the urea linker, resulting in compound **10**. Binding to the

ribosome for **10** was marginally improved (2.24 µg/ml), although at the MIC level (12.5 µg/ml)

10 was much more active than **8** (>200 µg/ml). When **10** was tested against the Rv1258c KO, its

activity improved further (3.1 µg/ml) indicating that the constraints of the urea linker may

interfere with efflux avoidance. To conclude the linker SAR, the influence of the length of the

spacer between the 3'-amide carbonyl bond to the pyridine ring in **1** was explored. Shortening of

the acetamide to a benzamide spacer (**11**) led to a decrease in ribosomal inhibition (7.19 µg/ml)

that was accompanied by a corresponding loss of antibacterial activity (MIC >200 µg/ml).

Increasing the length to a propanamide spacer (**12**) maintained ribosomal affinity (3.77 µg/ml),

but resulted in substantial loss of antibacterial potency (50 µg/ml). The MIC of **12** against the

Rv1258c KO improved 8 fold (6.3 µg/ml), indicating that increasing chain length increases

propensity for efflux by pump Rv1258c. These SAR results support our hypotheses that firstly,

the positioning the pyridyl ring nitrogen in the ribosomal pocket through correct spacer

orientation is key for optimum ribosomal binding enabling stabilizing hydrogen bonding

interactions; secondly, the spatial arrangement of 2-pyridyl relative to the spectinamide core is

key to efflux avoidance.

Table 1. Exploring the SAR of **1**: the effect of pyridyl nitrogen position (**1-4**) and the linker (**6-9**

and **10-12**).

Compound		H37Rv MIC (µg/ml)	Rv1258c KO MIC (µg/ml)	Efflux Ratio	Ribosome IC$_{50}$ (µg/mL)
SPC		100	6.3	16	0.36
1		1.6	3.1	0.5	1.01
2		50	1.6	32	3.02
3		200	6.3	32	5.07
4		200	12.5	16	4.75
5 (s-isomer)		>200	>200	-	42.23
6		200	ND	-	ND
7		>200	>200	-	16.62
8		>200	25	>8	3.77
9		>200	12.5	>16	10.97

10		12.5	3.1	4	2.24
11		>200	>200	-	7.19
12		50	6.3	8	3.80

Bioisosteric replacement with different heteroaryl ring systems

Bioisosteric replacement of the pyridyl side chain with other heterocylic ring systems was

examined with the purpose of further mapping SAR, finding new potential leads and providing

alternative scaffolds in case of the discovery of unwanted secondary pharmacology associated

with the 2-pyridyl side chain of **1** later in development.
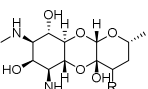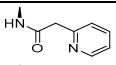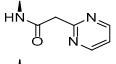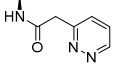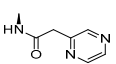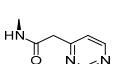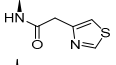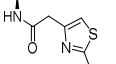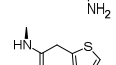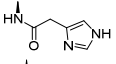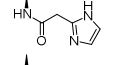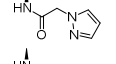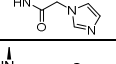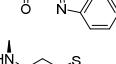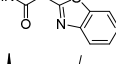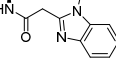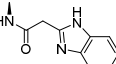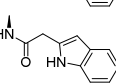
The addition of a second nitrogen to the ring of 2-linked pyridines produced interesting SAR.

The most pronounced change was observed with the 1,3 pyrimidine **13**, which has very poor

ribosomal activity (45.50 µg/ml, Table 2) and has no antitubercular activity, an observation that

is further explored in the molecular modeling section of this study. Pyridazine **14,** pyrazine **15,**

and pyrimidine **16** also had poor MIC activity (12.5-25 µg/ml), but in contrast to **13**, they are

potent ribosomal inhibitors (≤0.63 µg/ml). The MIC of these compounds did not improve

against the Rv1258c KO, indicating their poor activity is not due to efflux. With the exception of

13, the mechanistic reason for these results is unclear, but we hypothesize that putting the second

nitrogen in the ring may affect uptake or accumulation within the tuberculosis cell.

The second heterocyclic systems explored were the pyridine bioisosteres: 5-member ring

thiazole (4-yl) **17**, aminothiazole **18** and thiazole (2-yl) **19**; all compounds in this set were potent

ribosomal inhibitors (<1 µg/ml), with good antitubercular MIC values (≤6.3 µg/ml). These

results are consistent with the medicinal chemistry literature where pyridyl groups are commonly

replaced by similar sized thiazole rings. Introduction of smaller 5 member rings with 2 nitrogen

atoms including imidazoles **20**, **21**, **23** and pyrazole **22** produced analogs with a range of MIC

activities. 5-Imidazoyl **20** and 2-imidazoyl **21** had poor MIC values (25 and 12.5 µg/ml), despite

considerable ribosomal inhibition (1.10 and 0.56 µg/ml). These results suggest that uptake of

these compounds is limited by the increased basicity of the imidazole (pKa 7) ring over pyridyl

(pKa 5) which may disfavor permeation into cells or promote efflux by a separate pump. In this

sub-series, the requirement for a heteroaryl nitrogen adjacent to the linker to avoid efflux is

observed by comparison of the MIC active pyrazole **22** (6.3 µg/ml) and the MIC inactive

imidazole **23** (100 µg/ml), which is effluxed (8-fold).

Finally, a series of phenyl fused five-six member heteroaryl bicyclic ring systems that all retain

the key 2-linked aryl nitrogen were synthesized to determine if a larger group could be tolerated

both stereochemically and electrochemically at the back of the five member ring. The 2-linked

benzoxazole **24**, benzthiazole **25**, and benzimidazoles **26** / **27** all had very good MICs/ribosomal

inhibition and were not subject to efflux. Indole **28**, which has an NH instead of an N adjacent to

the linker position, however was subject to a very high efflux ratio (32 fold) with an MIC of 25

µg/ml. These results indicate the importance that the key heteroaryl nitrogen does not become

sufficiently basic to be protonated at physiological pH for MIC activity. This protonation state is

likely a contributing factor when comparing the MIC activities of the contrasting matched pair of

the weakly active imidazole **21** (pKa 7.0) and strongly active benzimidazole **27** (pKa 5.6).

Table 2. Examination of different heteroaryl ring systems

Compound		H37Rv MIC (µg/ml)	Rv1258c KO MIC (µg/ml)	Efflux Ratio	Ribosome IC$_{50}$ (µg/mL)
1		1.6	3.1	0.5	1.01
13		>200	>200	-	45.50
14		25	12.5	2	0.63
15		25	25	1	0.62
16		12.5	25	0.5	0.61
17		3.1	6.3	0.5	0.65
18		6.3	6.3	1	0.62
19		6.3	6.3	1	0.72
20		25	12.5	2	1.10
21		12.5	6.3	2	0.56
22		6.3	6.3	1	0.42
23		100	12.5	8	1.51
24		6.3	3.1	2	0.61
25		1.6	0.8	2	1.09
26		6.3	3.1	2	0.26
27		1.6	1.6	1	0.26
28		25	0.8	32	0.77

Introduction of electron donating/withdrawing group into the pyridine ring

The final component of SAR explored in this study is the effect of substitutions to the 2-linked

pyridine ring. Spectinamides were synthesized containing electron donating (ED) or electron

withdrawing (EW) substituents placed around the pyridyl ring in order to determine if

modulating the electrochemistry of the ring could fine tune either the ribosomal binding or efflux

avoidance (Table 3). All the compounds generated had good ribosomal inhibition (≤1 µg/mL).

In the first sub-series, a methyl group was introduced into each of the four free positions around

the 2-linked pyridyl ring. The addition of the methyl group to either the 3 (**29**) or 6 (**32**)

positions was not well tolerated due to an increased susceptibility of the compounds to efflux.

The 4 (**30**) and the 5 (**31**) substituted isomers had good MIC values suggesting that these are the

best positions for further modification. The substitution at the 4 position (**33-36**) has significant

effects on the chemistry of the critical pyridyl nitrogen. Compounds with electron donating

groups were not favored, having poor (12.5-25 µg/ml) MIC activity and were subject to mild

efflux. It is likely that **35** equilibrates to the corresponding 4-pyridone in which the pyridyl

nitrogen is protonated, which is consistent with prior SAR where the heteroaryl nitrogen is

protonated (**28** and **20**). The isopropyl substituted analog **33** had reasonable MIC activity (6.3

µg/ml), but was subject to mild efflux (4-fold). This suggests that introducing sterically larger

groups to this position can be tolerated, which is consistent with our molecular modeling

experiments. The 4-chloro substituted analog **36** was the most active in this subset, indicating

that electron withdrawing groups are favored in this position. Unfortunately, attempts to

synthesize the corresponding 4-fluoro analogs failed due to chemical reactivity of 4-

fluoropyridines to nucleophilic attack, which is also a concern for the 4-chloropyridine analogs.

The pharmacological implications in regard to safety and potential susceptibility to conjugative
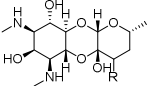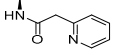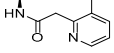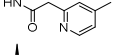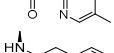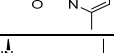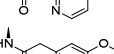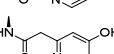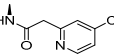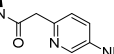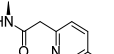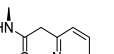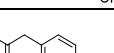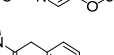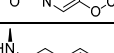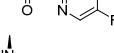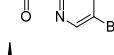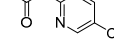
phase II metabolism with glutathione of 4-chloro substituted pyridines, is an issue we have recently evaluated in detail.[18]
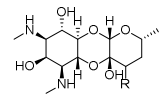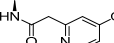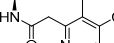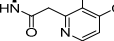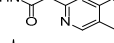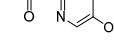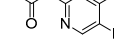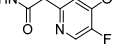
The 5-position is the most tolerant position for substitution and can be substituted with a variety of electron withdrawing and donating groups, all with good chemical stability. The MIC activity for all eight compounds (ED, **37-39**; EW, **40** and **41**; halogen, **42-44**) with mono substitution at this position was good, consistent with our modeling experiments that indicate that this position points largely away from the ribosome. The most notable compounds in this subset are the halogenated analogs **44**, **42**, **43** and hydroxyl analog **39**, all with excellent MIC values and the halogenated analogs all having long post antibiotic effects as discussed later (Table 5). The difference in MIC between 4 (**35**, 25 µg/ml) and 5 (**39**, 1.6 µg/ml) hydroxy substitutents is profound. Overall, the tolerability of this position to the introduction of different functional groups especially electron donating groups provides opportunity to perform further chemistry at the 5 position.

Dual substitutions to the pyridyl ring were explored (Table 4) using 4-chloro substituted **36** as a reference. Introduction of an isopropyl group at the 3-position led to a decrease in MIC activity (**45**, 50 µg/ml), due in part to a small loss of ribosomal inhibition (2.3 µg/ml), but most prominently due to increased efflux (32 fold). 4-chloro and 5 position dual substitution using methyl (**47**), methoxy (**48**), fluoro (**49**) produced compounds with excellent MIC and ribosomal inhibition that were not subject to efflux. As previously noted 4-chloro substituted pyridines are potentially chemically reactive, producing a concern that they may be subject to phase II conjugative metabolism. However, we have demonstrated that introduction of an electron withdrawing 5-fluoro group (**49**) can stabilize the 4-chloro group, while compounds with electron donating groups, such as **47** and **48** are more electrophilic and subject to metabolism.[18]

The final compound in this subset is **50**, a 4-methoxy and 5-fluoro substituted analog, essentially

a hybrid of **34** and **42**. Unfortunately, only moderate MIC activity was achieved, consistent with

the notion that an electron donating functional group in the 4-position is disfavored.

Table 3. Introducing electron donating/withdrawing group(s) into pyridine ring

Compound		H37Rv MIC (µg/ml)	Rv1258c KO MIC (µg/ml)	Efflux Ratio	Ribosome IC$_{50}$ (µg/mL)
1		1.6	3.2	0.5	1.01
29		25	6.3	4	1.00
30		3.1	6.3	0.5	0.47
31		3.1	3.1	1	0.54
32		25	6.3	4	0.50
33		6.3	1.6	4	0.36
34		12.5	3.1	4	0.39
35		25	12.5	2	0.44
36		1.6	1.6	1	0.54
37		6.3	6.3	1	0.30
38		3.1	6.3	0.5	0.39
39		1.6	3.1	0.5	0.84
40		3.1	1.6	2	0.44
41		3.1	0.8	4	0.96
42		1.6	3.1	0.5	0.55
43		3.1	1.6	2	0.42
44		0.8	0.8	1	0.53

Table 4. Introducing dual groups into pyridine ring

Compound		H37Rv MIC (µg/ml)	Rv1258c KO MIC (µg/ml)	Efflux Ratio	Ribosome IC$_{50}$ (µg/mL)
36		1.6	1.6	1	0.54
45		50	1.6	32	2.31
46		3.1	1.6	2	0.59
47		0.8	0.8	1	0.23
48		3.1	3.1	1	0.42
49		0.8	0.8	1	0.22
50		6.3	3.1	2	0.92

Ribosome SAR summary

The ribosomal SAR observed with respect to substitution of the aryl sidechain to the 3' position

of the spectinomycin ring largely rests on positioning the 2-pyridyl ring correctly in the binding

site. First, chirality of the ring substitution is absolute with only 3' (R) amides active. Linker

length and type is also key in positioning the side chain ring to make optimum interactions. A

shorter linker such as **11** or alternatives such as carbamate (**7**) or sulfonamide (**9**) were

disfavored. The position of the linker to nitrogen in the pyridyl ring also had a significant effect,

with the 2-linked series being optimum. In terms of substitution to the pyridyl ring the most

dramatic loss in affinity was generated by the addition of a second nitrogen adjacent to the linker

(**13**). The remainder of the compounds were designed to fit within the envelope of the

spectinamide side chain binding site formed adjacent to helix 34 and below RpsE interaction

loop, details of which are discussed in greater detail in the subsequent molecular modeling

section.

Efflux SAR summary

In regard to the key element of SAR – efflux avoidance, critical to the success of this series is the

presence of a non-protonated heterocyclic nitrogen immediately adjacent to linker to the

spectinomycin core. Within these tables there are several examples (**1** vs **2, 8** vs **10, 22** vs **23)**

that if the key nitrogen is replaced, MIC activity is adversely affected in wild type *M.*

tuberculosis but the MIC activity is retained in the tuberculosis strain in which the Rv1258c

efflux pump has been deleted. The need for non-protonated heterocyclic nitrogen (N not NH) to

avoid efflux is also clearly demonstrated in the **27** and **28** pair.

Within this requirement, different heteroaryl rings are well tolerated providing opportunities to

expand the series and manipulate potential off-target pharmacologic effects. Steric and

electronic substitutions to the heteroaryl (pyridyl) ring alter the propensity of compounds in this

series to avoid efflux. Electron donating substitutions to the 4-position of the pyridyl ring

increase the propensity for efflux and decrease MIC activity. Conversely, introduction of 4-

position of electron withdrawing substitutions appears favorable with the caveat of introduction

of potential chemical instability.   Modifications to the 3 and 6 positions appear sterically

unfavorable as evidenced by **29**, **32**, and **45**, potentially indicating that there is a biochemical

recognition element to efflux avoidance. Substitutions to the pyridyl 5 position are broadly

tolerated in respect to the efflux SAR and may be coupled with 4-position substitutions to

produce potent dual substituted compounds such as **49**. To ensure no MIC biases were

accidentally introduced in the creation of Rv1258c KO strain, a complemented strain in which

the Rv1258c pump was reintroduced to the KO strain was used as a control. All MICs of the

compounds in this series against the complemented strain were within one well of the H37Rv

wild type parental strain indicating that the efflux effects noted in this manuscript were specific

to the Rv1258c pump.

Modeling

To understand the structure-activity relationship with respect to ribosome affinity, key

compounds were docked into the active site and then subjected to a 20 ns molecular dynamics

simulation. These experiments were directed at understanding how small modifications on the

aryl side chain can affect binding affinity, such as observed with the improvement in activity

with side chains from benzyl (**2**) to pyridyl (**1**) and to 4-chloropyridyl (**36**). In the case of **2**, the

benzene ring remained significantly more dynamic than **1** whose pyridyl nitrogen provided a

possibility for a hydrogen bond that stabilized the ring in the simulations and increased the

predicted binding affinity by 0.7 kcal/mol. With two possible hydrogen bonding partners

(C1192, G1193) (Figure 2A and C), the pyridine ring however did not adopt a single pose in the

20 ns production run. Compound **13** (IC_{50}=45.5 µM) with two nitrogens bound 39 fold weaker

than **1** with a calculated relative binding free energy of 2.21 kcal/mol. (Table S2). The

decomposed energy terms suggested that both the electrostatic and non-polar component of the

relative ΔG_{bind} was less favorable than reference compound **1**. To rationalize this, we calculated

the Donor-Acceptor (D-A) distances between the two nitrogen atoms on the ring and

G1193/C1192. Using a D-A cut-off distance of 4.0 Å and a cut-off angle of 60° for H-D-A,

hydrogen bond with C1192 was present only 11% of the time, and the interaction with G1193

was even weaker. Thus with the addition of the second nitrogen, the pyrimidine did not establish

a second favorable interaction. A likely explanation is that the two hydrogen bonds competed

with each other in **13** resulting in an overall weaker hydrogen bond and disfavored interaction

with the lipophilic RpsE residues at the back of the aryl binding pocket.

Adding a chlorine to the pyridine ring (**36**) allowed an additional favorable interaction between

the halogen and amide backbone of F30, and in conjunction with hydrogen bonding of the

pyridyl nitrogen and G1193, locked the ring movement in the simulation (Figure 2 B and D).

This increased binding affinity by a predicted 0.5 kcal/mol. It is tempting to speculate that this is

the reason that the halogenated pyridines such as **36** possess long post antibiotic effects as

discussed further in the next section, though experimentally, residence time determinations are

hard to perform on such a complex macromolecular system as the bacterial ribosome.
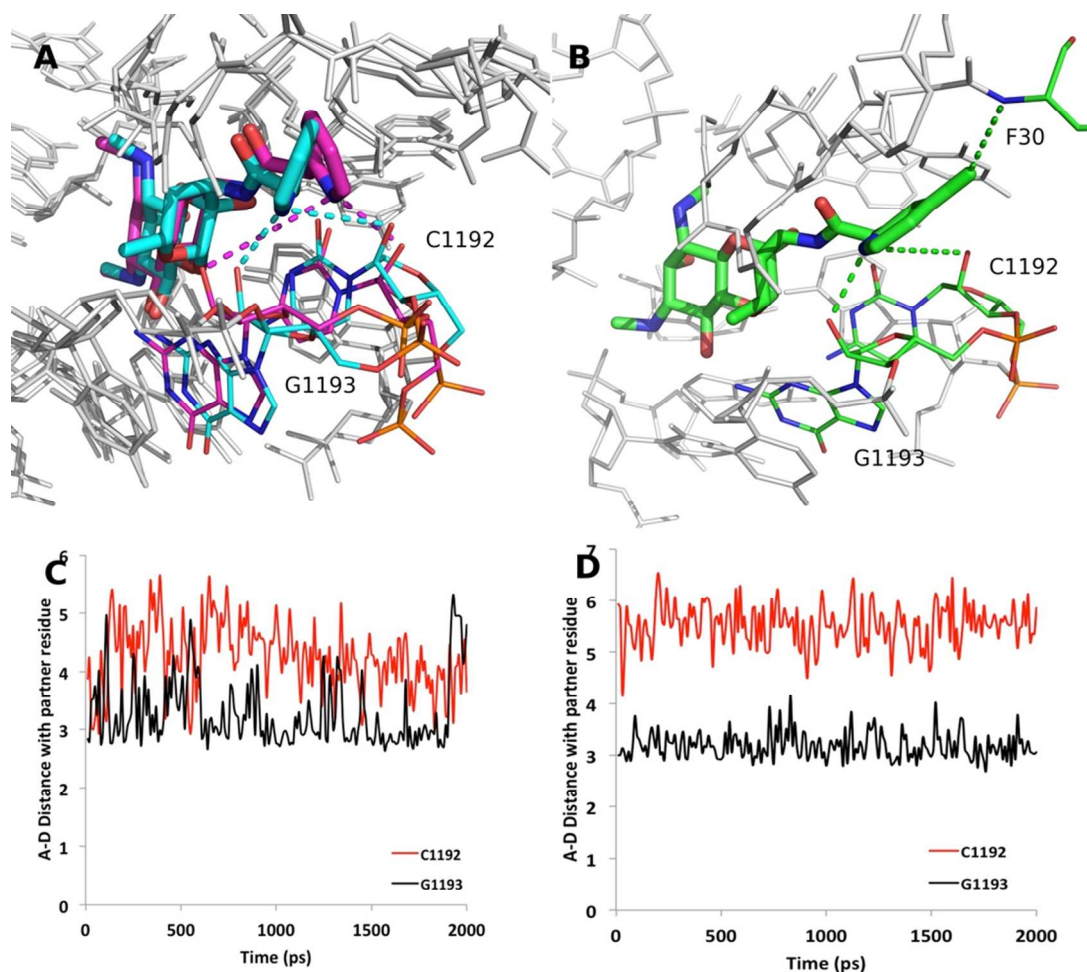
Figure 2. Snapshots taken from the last 20ns MD trajectory for **1** (A) and **36** (B). The two possible hydrogen bonding interactions made by **1** are shown in magenta and teal (A).The Acceptor-Donor (A-D) distances (in Å) between the pyridine Nitrogen and G1193 and C1192 plotted for **1** (C) and **36** (D).

Post antibiotic effect.

While MIC is an important parameter used in the development of antibacterial compounds, it observes antimicrobial activity with static drug exposure unrepresentative of the oscillating exposures encountered by a pathogen *in vivo*. Metabolism and clearance of compounds *in vivo*
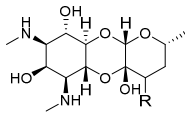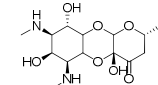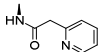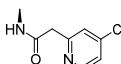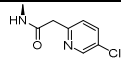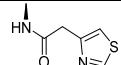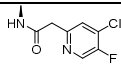
results in a transient period of time in which a compound must exert an effect sufficient to kill and suppress bacterial re-growth until the next dose is administered. For injectable compounds with relatively short *in vivo* half-lives, such as the spectinomycin,[19] we anticipated this is could be an important driver of *in vivo* efficacy. As a way to prioritize compounds for later resource and time intensive *in vivo* efficacy experiments, we performed post antibiotic effect (PAE) experiments *in vitro* using *M. bovis* BCG as a safer tuberculosis surrogate (Table 5). Within the limited number of compounds tested, a clear SAR was observed; unsubstituted pyridyl and thiazole analogs, **1** and **17**, exhibited moderate PAEs (23-27 hrs), whereas analogs with halogenated substitutions, **47**, **49**, **49** and **44**, exerted a lengthy PAE that exceeded 100 hours. The PAE of the hydroxyl analog **39** (20 hours) was lower that the corresponding halogens. These results are consistent with the previous molecular dynamics experiments, which predict enhanced ribosomal residency times of the halogenated spectinamides.
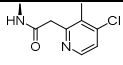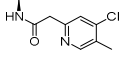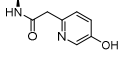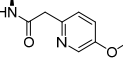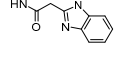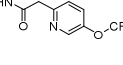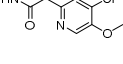
In vitro ADME profiling

Select lead compounds were subject to further pharmacological profiling, including *in vitro* testing of cytotoxicity, microsomal stability, protein binding; all key factors when evaluating potential antibiotic substances for further advancement. Consistent with our previously published studies on **44**, **36** and **1**, all the new spectinamides tested in these experiments exhibited no apparent cytotoxicity to HepG2 cells (all >400 µg/mL). The stability to both human and mouse microsomal metabolism was also excellent for most compounds in the series. All compounds in the series had a human microsomal half-life ≥6.3 h, except for **36** and **38**, indicative of low phase I hepatic metabolic potential for the series. As we have noted previously, **47** and **36** are subject

to some phase II conjugative metabolism.[18] Protein serum binding was low for all compounds

with the lowest levels for **39** (35%) and highest for **49** (56%), which is consistent with increasing

lipophilicity of the pyridyl substitutions. The negligible toxicity towards mammalian cells, low

propensity for phase I metabolism, low protein binding and high solubility are shown here to be

a clear and desirable general properties of this antibiotic class.

Table 5. *In vitro* ADME, PAE and cytotoxicity testing of selected series leads.

#		MIC (H$_{37}$Rv) (µg/mL)	Post Antibiotic Effect^ (h)	Microsomal stability t1/2(h)		Protein binding (%)		Cytotoxicity (HepG2) (µg/mL)
				human	mouse	human	mouse	
SPC*		100	-	2.5	>10	51.6	52.6	>400
1*		1.6	23 (8)	>10	>10	62.1	36.9	>400
36*		1.6	66 (29)	2.6	1.5	56.4	39.8	>400
44*		0.8	133 (26)	21.2	>50	-	29.8	>400
17*		3.1	27 (13)	18.5	5.6	52.4	41.6	>400
49		0.8	116 (19)	>50	>50	56.3	39.3	>400

46		3.1	-	>50	>50	46.6	36.4	>400
47		0.8	102 (15)	>50	>50	43.9	42.7	>400
39		1.6	20 (18)	7.4	13.4	35.1	30.7	>400
38		3.1	56 (12)	3.4	4.8	51.4	57.3	>400
27		1.6	137	>50	>50	26.3	12.1	>400
41		3.1	61 (17)	22.4	27.0	51.4	58.4	>400
48		3.1	72 (10)	6.3	5.5	61.6	72.9	>400

^ Results of Post-Antibiotic Effect experiments are presented (in hours) as the average of 2-3 biologically independent replicates, with standard deviation indicated in parenthesis using *M. bovis* BCG. * previously reported in ref 4,

In vivo **efficacy**

To acertain if there was any notable difference in the *in vivo* efficacy or tolerability in relation to the selection of the spectinamide side chain, key spectinamides were tested in a mouse model of acute tuberculosis infection (Figure 3 A-C) and for their maximum tolerated dose (Table S3). Data shown here results from two new separate trials (Figure 3B and 3C, Table S4) with the spectinamides being dosed at 200mg/kg twice daily (BID) for 9 days unless otherwise noted. These data can be compared with our previous trial with **1**, **42**, **36**, **44** performed in identical

manner (Figure 3A). However, it must be noted that comparative significance can only be studied within individual trials as bacterial loads often differ between trials.

In the first new trial, three representative heteroaryl compounds with low MICs and excellent ribosomal inhibition (thiazole **17,** benzothiazole **25** and benzimidazole **27**) were chosen to determine if the pyridyl group could be replaced without penalty, and three dual-substituted 4-chloro analogs with low MICs and excellent ribosomal inhibition (**49**, **47**, and **46)** were chosen to see if dual substitution was advantageous. From this group, benzothiazole **25** was excluded due to mild toxicity noted when dosage exceeded 100 mg/kg during preliminary maximum tolerated dose testing. Both **17** and **27** reduced the bacterial load in mice with dosing at 200 mg/kg BID by 1.6 logs. Treatment with 3- methyl substituted **46** produced the least reduction in bacterial loads, while 5- substituted analogs **49** and **47** both exerted more than 2 logs of bacterial killing. Perhaps the most notable result from this trial was that the efficacy of **49** was comparable to the clinically used antitubercular, streptomycin, which was adminstered using the same dosing strategy.

In the second new efficacy trial, compounds **41**, **39**, **38**, **48** were tested to explore the SAR of non-halogen electron donating groups in the 5-position. Compound **41**, the 5- trifluoromethoxy substituted analog, exerted lowest antibacterial activity (1.1 log reduction in lungs). Two of the most potent analogs in terms of MIC, **39** and **38**, yielded 1.5 and 1.6 logs of killing. **48** (the 4-chloro 5-methoxyl analog) yielded a 1.6 log reduction in pulmonary load, similar to that of streptomycin in this trial (l.6 log CFU reduction). These results suggest that switching the 5-substitution between electron withdrawing (**42**, Figure 3A) and electron donating (**39** and **38**) substitutions have little effect on the *in vivo* efficacy in this model. It should also be noted that the BID dosing schedule used in this trial might negate the effects of the prominent differences in PAE between compounds with this substitution which may be more likely to be observed in long

term efficacy trials of chronic infection using once daily dosing 5 days a week.[20]   Previous

pharmacokinetic testing on 1, 42, 36, and 44, demonstrated that compounds in this class share

similar profiles with short half-lives (0.44-1.0h) dictated by renal clearance.[4] This is driven by

the spectinomycin core rather than the spectinamide sidechain, with exposures similar to

aminoglycoside antibiotics.[16]

The results of the new efficacy trials were similar to our prior studies (Figure 3A). All new

analogs tested (Figure 3B and 4C) demonstrated statistically significant *in vivo* efficacy in

reducing bacterial burden in lungs of gamma-interferon KO mice when compared to saline

controls ($P < 0.001$), showing more than one $\log_{10}$CFU reduction versus the control after nine

consecutive days of treatment. All compounds with the exception of **41** (100 mg/kg) were well

tollerated at a dosing of 200 mg/kg (Table S3). The most active compounds generally were

those with the lowest MIC values. The stand out compounds were **49,** with potency equivalent

to that of streptomycin when administered at the same dose ($P > 0.05$), and **39**, the compound

that was tolerated the best, with a maximum tolerated dose (MTD) >400 mg/kg in mice. These

results show that there are many bioiosteric ring choices for the spectinamide side chain, which

may be useful should adverse events be found associated with specific side chains.
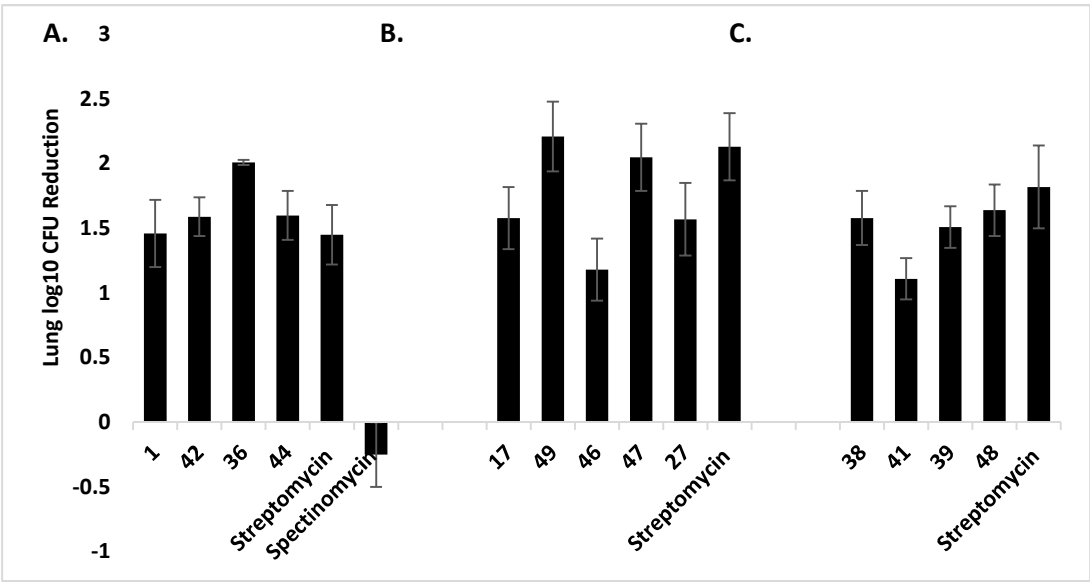
Figure 3. Efficacy of spectinamides in a gamma interferon KO mouse model of acute

tuberculosis infection. Results are from three separate experiments (A)[4], (B) and (C) and show

the reduction in lung CFU counts in comparison to PBS injected control. The reduction of

bacterial load in lungs of infected mice was calculated as the difference between the vehicle

carrier injected control group and groups treated for 9 days with streptomycin or experimental

compounds. Groups of 4-7 mice were administered treatment doses at 200 mg/Kg twice daily,

execpt **41** at 100 mg/Kg. Error bars indicate the SEM.

Activity against drug resistant clinical *M. tuberculosis* isolates

To further confirm **49** and **39** as viable candidates, MIC testing was performed against a panel of

29 clinical isolates, including 18 MDR and 5 extensively drug resistant isolates (Table S5). The

MIC$_{90}$, the lowest concentration of the antibiotic at which 90% of the isolates were inhibited, and

MIC range in this panel for **49** was 0.78 (0.39-1.56) and **39** was 3.13 (1.56-3.13), both

impressively narrow. These results indicate a low potential of cross resistance to exisiting drugs,

similar to our current lead **44**.

CONCLUSION

The structure activity relationships detailed in this manuscript provides further insight into the important role efflux plays in intrinsic antibiotic resistance in tuberculosis. The ability to understand the structural rules for the spectinamide class has produced a variety of substituted 2-N-heteroaryl linked spectinamides with proven *in vivo* efficacy. Having a 2-N-heteroaryl motif hydrogen bond donor is essential for evading Rv1258c mediated efflux modulating activity. Computational studies show modifications to the 2 linked pyridyl ring help lock orientation of the aryl ring in a desirable position in the ribosome, corresponding to the long PAE in 4 and 5 halogenated analogs. These key computational and SAR findings should enable further rounds of inhibitor design. Based on IC_{50}, potency, and efficacy data, **49** (MIC potency, metabolic stability and long post antibiotic effect) and **39** (MIC potency, high tolerability) could be potential antituberculosis drug candidates for further pre-clinical evaluation providing alternatives therapeutic to current lead **44** for the development of this class of antitubercular agents. Studies are currently ongoing to examine the mechanism of uptake of the spectinamide series, synergy mechanisms with other antituberculosis agents such as rifampin and pyrazinamide, and the ability of these agents to partner with other tuberculosis experimental therapeutics to shorten tuberculosis treatment times for MDR-tuberculosis.

EXPERIMENTAL SECTION

Spectinomycin dihydrochloride pentahydrate was purchased from Waterstone Technology

(catalog number 81249, CAS number 22189-32-8, 95% in purity). All solvents used for

chromatography and liquid chromatography were purchased from Aldrich. Flash column

chromatography silica cartridges were obtained from Biotage Inc. Reactions were monitored by

thin-layer chromatography (TLC) on pre-coated Merch 60 F254 silica gel plates and visualized

using UV light (254 nm). A Biotage FLASH column chromatography system was used to purify

mixtures. ^{1}H NMR spectra were recorded on a Varian INOVA-500 spectrometer or on a Bruker

400 MHz NMR spectrometer. Chemical shifts (δ) are reported in parts per million relative to the

residual solvent peak or internal standard (tetramethylsilane), and coupling constants (J) are

reported in hertz (Hz). High resolution mass spectra were recorded on a Waters Xevo G2 QTOF

LC–MS using ESI. Purity of the products was confirmed by UPLC/MS (the Waters Acquity).

Elemental analysis was tested by Atlantic Microlab Inc. X-ray was analyzed on Bruker D8

diffractometer.

Synthesis of 1, 3-Bis (N-benzyloxycarbonyl)-spectinomycin:

The title compound was synthesized according to the procedure described in the Journal of

Organic Chemistry.[21]

Synthesis of 1, 3-Bis (N-benzyloxycarbonyl)-3'-dihyro-3'-deoxy-3'(R)-aminospectinomycin:

1, 3-Bis (N-benzyloxycarbonyl)-spectinomycin (6.6g, 11mmol) and NH_4NO_3 (8.8g, 110mmol) in

100mL of 10% acetic acid-methanol were stirred to clear solution at room temperature. 2-

Methylpyridine borane (0.82g, 7.7mmol) was added to the reaction mixture in one portion. The

mixture was stirred for 1 h at room temperature and the solvent evaporated. The residue was

dissolved into 100mL saturated $NaHCO_3$ solution and 100mL ethyl acetate.

After separation, the organic layer was washed with brine and dried over Na_2SO_4. After

evaporating the solvent, 2.6g (40%) title compound was purified by column chromatography

(Isolera one, Biotage, HP column, 50g size, 5% methanol/acetonitrile).[15] ^{1}H NMR (400 MHz,

Methanol-d_4) δ 7.46 – 7.19 (m, 10H), 5.30 – 4.98 (m, 4H), 4.91 (s, 1H), 4.53 (t, J = 10.5 Hz,

1H), 4.24 – 3.82 (m, 7H), 3.18 – 3.01 (m, 6H), 1.92 – 1.77 (m, 1H), 1.68-1.61 (m, 1H), 1.25 (d, J

= 5.9 Hz, 3H). MS-ESI: m/z 602 (M^++H).

General methods to make spectinamides:

 Amine (1 equivalent), acid (1.1 equivalent) and HBTU (1.1 equivalent) were dissolved into

CH_2Cl_2 or DMF. The mixture was stirred at room temperature for 10 minutes. The reaction was

quenched by water. The organic layer was collected after separation, then washed by water and

brine, dried (Na_2SO_4) and evaporated. The residue was purified by column chromatography

(10% ethyl acetate/methanol) and was then ready for deprotection.

Deprotection Method 1: Hydrogenation. The Cbz compound was dissolved into 1.25 M

HCl/MeOH and Cbz groups were removed by catalytic hydrogenation using palladium on carbon

(10% Pd/C) for 2 hrs. Removal of catalyst, concentration and trituration with ether afforded the

spectinamide with hydrochloride salts.

Deprotection Method 2: Hydrolysis. The Cbz compound was dissolved into 48% HBr solution

and Cbz groups were removed by acid at room temperature for 2hs. The reaction mixture was

triturated with acetone, filtered and washed with acetone again to yield spectinamide as the

hydrobromide salt.

3'-Dihydro-3'-deoxy-3'(R)-(pyridin-3yl)acetylamino spectinomycin trihydrochloride (3):

Method 1, Yield: 67%. ^{1}H NMR (D$_2$O, 500 MHz): δ 8.80-8.70 (m, 2H), 8.56-8.50 (m, 1H), 8.07 (dd, J = 7.5, 6.0 Hz, 1H), 5.02 (s, 1H), 4.40 (t, J = 10.5 Hz, 1H), 4.19 (t, J = 3.5 Hz, 1H), 4.14-3.94 (m, 6H), 3.52 (dd, J = 11.0, 2.5 Hz, 1H), 3.27 (dd, J = 10.0, 2.5 Hz, 1H), 2.83 (s, 3H), 2.82 (s, 3H), 1.96-1.86 (m, 1H), 1.80-1.70 (m, 1H), 1.26 (d, J = 6.0 Hz, 3H). HRMS-ESI calcd for C$_{21}$H$_{32}$N$_4$O$_7$ [M+H]$^+$ 453.2349, found: 453.2354.

3'-Dihydro-3'-deoxy-3'(R)-pyridin-2-carboxylicamino spectinomycin trihydrochloride (11):

Method 1, Yield: 52%. ^{1}H NMR (D$_2$O, 500 MHz): δ 8.66 (d, J = 4.5 Hz, 1H), 8.10 (d, J = 3.5 Hz, 2H), 7.74-7.65 (m, 1H), 5.16 (s, 1H), 4.45 (t, J = 11.0 Hz, 1H), 4.39 (t, J = 3.5 Hz, 1H), 4.25-4.15 (m, 1H), 4.07 (t, J = 10.0 Hz, 1H), 4.00 (t, J = 10.5 Hz, 1H), 3.56 (dd, J = 11.0, 2.5 Hz, 1H), 3.28 (dd, J = 10.0, 2.5 Hz, 1H), 2.86 (s, 3H), 2.84 (s, 3H), 2.02-1.98 (m, 1H), 1.97-1.91 (m, 1H), 1.28 (d, J = 6.0 Hz, 3H. HRMS-ESI calcd for C$_{20}$H$_{31}$N$_4$O$_7$ [M+H]$^+$ 439.2193, found: 439.2188.

3'-Dihydro-3'-deoxy-3'(R)-(pyridin-4yl)acetylamino spectinomycin trihydrochloride (4):

Method 1, Yield: 62%. ^{1}H NMR (D$_2$O, 500 MHz): δ 8.71 (t, J = 6.3 Hz, 2H), 7.97 (d, J = 5.8 Hz, 1H), 7.89 (d, J = 6.1 Hz, 1H), 4.99 (s, 1H), 4.36 (t, J = 10.0 Hz, 1H), 4.17 (d, J = 10.9 Hz, 1H), 3.92-4.18 (m, 3H), 3.62 (q, J = 7.0 Hz, 1H), 3.50 (d, J = 10.9 Hz, 1H), 3.41 (d, J = 11.9 Hz, 1H), 3.24 (d, J = 9.7 Hz, 1H), 2.96-3.02 (m, 1H), 2.81 (s, 6H), 1.86-1.89 (m, 1H), 1.64-1.74 (m, 1H), 1.23 (d, J = 5.3 Hz, 3H. HRMS-ESI calcd for C$_{21}$H$_{33}$N$_4$O$_7$ [M+H]$^+$ 453.2349, found: 453.2354.

3'-Dihydro-3'-deoxy-3'(R)-(pyridin-4yl)acetylamino spectinomycin trihydrochloride (4):

Method 1, Yield: 62%. ^{1}H NMR (D$_2$O, 500 MHz): δ 8.71 (t, J = 6.3 Hz, 2H), 7.97 (d, J = 5.8 Hz, 1H), 7.89 (d, J = 6.1 Hz, 1H), 4.99 (s, 1H), 4.36 (t, J = 10.0 Hz, 1H), 4.17 (d, J = 10.9 Hz, 1H),

3.92-4.18 (m, 3H), 3.62 (q, J = 7.0 Hz, 1H), 3.50 (d, J = 10.9 Hz, 1H), 3.41 (d, J = 11.9 Hz, 1H),

3.24 (d, J = 9.7 Hz, 1H), 2.96-3.02 (m, 1H), 2.81 (s, 6H), 1.86-1.89 (m, 1H), 1.64-1.74 (m, 1H),

1.23 (d, J = 5.3 Hz, 3H. HRMS-ESI calcd for $C_{21}H_{33}N_4O_7$ [M+H]$^+$ 453.2349, found: 453.2354.

3'-Dihydro-3'-deoxy-3'(S)-(pyridin-2-yl)acetylamino spectinomycin Trihydrobromide (5).

Method 2, Yield: 66%. ^{1}H NMR (400 MHz, D$_2$O) δ 8.75 (ddd, J = 0.76, 1.72, 5.88 Hz, 1H), 8.55

(td, J = 1.65, 7.96 Hz, 1H), 8.02 – 7.92 (m, 2H), 4.87 (s, 1H), 4.33 (dd, J = 9.80, 11.06 Hz, 1H),

4.25 (dd, J = 4.81, 12.55 Hz, 1H), 4.21 (d, J = 4.74 Hz, 1H), 4.10 – 3.89 (m, 3H), 3.60 (dd, J =

2.73, 11.03 Hz, 1H), 3.30 (dd, J = 2.87, 10.17 Hz, 1H), 2.88 (s, 3H), 2.85 (s, 3H), 1.87 – 1.80 (m,

1H), 1.63 (td, J = 11.26, 12.85 Hz, 1H), 1.28 (d, J = 6.08 Hz, 3H). HRMS-ESI calcd for

$C_{21}H_{33}N_4O_7$ [M+H]$^+$ 453.2349, found: 453.2355.

3'-Dihydro-3'-deoxy-4(R)-2-phenylethylamino spectinomycin trihydrochloride (6): Method

1, Yield: 53%. ^{1}H NMR (D$_2$O, 400 MHz): δ 7.32-7.42 (m, 3H), 7.22-7.29 (m, 2H), 5.01 (s, 1H),

4.38 (dd, J = 13.1 Hz, 2H), 4.28 (t, J = 10.5 Hz, 1H), 4.00-4.09 (m, 3H), 3.94 (t, J = 10.0 Hz,

1H), 3.50 (d, J = 10.9 Hz, 1H). 3.42 (br s, 1H), 3.25 (d, J = 10.0 Hz, 1H), 2.77 (m, 3H), 2.62 (s,

2H), 2.35 (s, 3H), 2.06 (d, J = 15.8 Hz, 1H), 1.95 (t, J = 11.7 Hz, 1H), 1.27 (d, J = 5.8 Hz, 3H).

MS-ESI: m/z 438 (M$^+$+H).

3'-Dihydro-3'-deoxy-3'(R)- phenyloxycarbonylamino spectinomycin dihydrochloride (7):

Method 1, Yield: 92%. ^{1}H NMR (400 MHz, D$_2$O) δ 7.43 (t, J = 7.7 Hz, 2H), 7.30 (t, J = 7.2 Hz,

1H), 7.13 (d, J = 7.7 Hz, 2H), 4.42 – 4.34 (m, 1H), 4.15 – 3.90 (m, 5H), 3.50 (dd, J = 11.1, 2.5

Hz, 1H), 3.32 (s, 1H), 3.26 – 3.19 (m, 1H), 2.80 (s, 6H), 1.97 – 1.72 (m, 2H), 1.25 (d, J = 5.9 Hz,

3H). HRMS-ESI calcd for $C_{21}H_{32}N_3O_8$ [M+H]$^+$ 454.2189, found: 454.2199.

3'-Dihydro-3'-deoxy-3'(R)- phenylaminocarbonylamino spectinomycin trihydrobromide

(8): Method 1, Yield: 89%. ^{1}H NMR (400 MHz, D$_2$O) δ 7.34 (t, J = 7.7 Hz, 2H), 7.26 (d, J = 8.0

Hz, 2H), 7.12 (t, J = 7.1 Hz, 1H), 4.88 (s, 1H), 4.71 (s, 1H), 4.37 (t, J = 10.4 Hz, 1H), 4.07 – 3.88

(m, 4H), 3.49 – 3.46 (m, 1H), 3.22 (dd, J = 10.0, 2.3 Hz, 1H), 2.79 (s, 3H), 2.78 (s, 3H), 1.94 –

1.83 (m, 1H), 1.77 (d, J = 14.3 Hz, 1H), 1.22 (d, J = 6.0 Hz, 3H). HRMS-ESI calcd for

$C_{21}H_{33}N_4O_7$ $[M+H]^+$ 453.2349, found: 453.2341.

3'-Dihydro-3'-deoxy-3'(R)- benzylsulfonylamino spectinomycin dihydrobromide (9):

Method 2, Yield: 65%. ^{1}H NMR (400 MHz, D_2O) δ 7.39 (s, 5H), 4.77 (s, 1H), 4.66 (d, J = 2.8

Hz, 1H), 4.46 (q, J = 14.0 Hz, 2H), 4.32 – 4.24 (m, 1H), 4.00 – 3.82 (m, 3H), 3.60 (d, J = 3.2 Hz,

1H), 3.41 (dd, J = 11.1, 2.7 Hz, 1H), 3.16 (dd, J = 9.9, 2.8 Hz, 1H), 2.73 (s, 6H), 1.82 – 1.70 (m,

1H), 1.45 (d, J = 14.6 Hz, 1H), 1.12 (d, J = 6.1 Hz, 3H). HRMS-ESI calcd for $C_{21}H_{34}N_3O_8S$

$[M+H]^+$ 488.2067, found: 488.2067.

3'-Dihydro-3'-deoxy-3'(*R*)-(pyridin-2-yl)aminocarbonylamino spectinomycin

dihydrochloride (10): Method 1, Yield: 52%. ^{1}H NMR (MeOH-d_4) δ 8.25 (ddd, J = 5.2, 1.9,

0.9 Hz, 1H), 7.73 (ddd, J = 8.4, 7.3, 1.9 Hz, 1H), 7.12 (d, J = 8.4 Hz, 1H), 7.01 (ddd, J = 7.3, 5.1,

1.0 Hz, 1H), 4.82 (s, 1H), 4.29 – 4.23 (m, 2H), 4.09 (t, J = 3.1 Hz, 1H), 3.94 (t, J = 9.8 Hz, 1H),

3.67 (t, J = 9.9 Hz, 1H), 3.04 (s, 1H), 2.90 (s, 1H), 2.61 – 2.57 (m, 1H), 2.55 – 2.52 (m, 1H), 2.52

– 2.46 (m, 6H), 2.45 – 2.41 (m, 1H), 1.96 – 1.89 (m, 2H), 1.29 (d, J = 6.1 Hz, 3H). HRMS-ESI

m/z = calculated 454.2302 $[M+H]^+$ found 454.2299.

3'-Dihydro-3'-deoxy-3'(R)-pyridin-2-carboxylicamino spectinomycin trihydrochloride

(11): Method 1, Yield: 52%. ^{1}H NMR (D_2O, 500 MHz): δ 8.66 (d, J = 4.5 Hz, 1H), 8.10 (d, J =

3.5 Hz, 2H), 7.74-7.65 (m, 1H), 5.16 (s, 1H), 4.45 (t, J = 11.0 Hz, 1H), 4.39 (t, J = 3.5 Hz, 1H),

4.25-4.15 (m, 1H), 4.07 (t, J = 10.0 Hz, 1H), 4.00 (t, J = 10.5 Hz, 1H), 3.56 (dd, J = 11.0, 2.5 Hz,

1H), 3.28 (dd, J = 10.0, 2.5 Hz, 1H), 2.86 (s, 3H), 2.84 (s, 3H), 2.02-1.98 (m, 1H), 1.97-1.91 (m,

1H), 1.28 (d, J = 6.0 Hz, 3H. HRMS-ESI calcd for $C_{20}H_{31}N_4O_7$ [M+H]$^+$ 439.2193, found: 439.2188.

3'-Dihydro-3'-deoxy-3'(R)-(pyridin-2-yl)propanoylamino spectinomycin trihydrobromide

(12): Method 2, Yield: 88%. ^{1}H NMR (400 MHz, D2O): δ 8.60 – 8.56 (m, 1H), 8.45 (td, J = 8.0 Hz, 1.6 Hz, 1H), 7.88 – 7.82 (m, 2H), 4.84 (s, 1H), 4.76 (s, 1H), 4.29 (dd, J = 10.9, 9.8 Hz, 1H), 4.03 (d, J =2.9 Hz, 1H), 3.98 – 3.81 (m, 3H), 3.44 (d, J = 11.2 Hz, 1H), 3.29 (dd, J = 11.6, 4.5 Hz, 2H), 3.22 – 3.15 (m, 1H), 2.83 (dd, J = 10.2, 4.4 Hz, 2H), 2.75 (s, 6H), 1.83 – 1.73 (m, 1H), 1.52 (d, J = 14.6 Hz, 1H), 1.14 (d, J = 6.1 Hz, 3H). HRMS-ESI calcd for $C_{22}H_{35}N_4O_7$ [M+H]$^+$ 467.2506, found: 467.2502.

3'-Dihydro-3'-deoxy-3'(R)-(pyrimidin-2yl)acetylamino spectinomycin dihydrochloride

(13): Method 1, Yield: 56%. ^{1}H NMR (D$_2$O, 500 MHz): δ 8.27 (d, J = 7.5 Hz, 1H), 7.99 (d, J = 6.35 Hz, 1H), 7.00 (t, J = 7.0 Hz, 1H), 5.06 (s, 1H), 4.35-4.43 (m, 2H), 4.00-4.08 (m, 2H), 3.89-3.98 (m, 1H), 3.54 (dd, J = 10.9 Hz, 2H), 3.43-3.46 (m, 1H), 3.35-3.40 (m, 1H), 3.25 (t, J = 6.3 Hz, 1H), 2.82 (s, 6H), 2.14-2.15 (m, 2H), 1.25 (d, J = 5.6 Hz, 3H); HRMS-ESI calcd for $C_{20}H_{32}N_5O_7$ [M+H]$^+$ 454.2302, found: 454.2301.

3'-Dihydro-3'-deoxy-3'(R)-(pyridazin-3-yl) acetylamino spectinomycin trihydrobromide

(14): Method 2, Yield: 28%. ^{1}H NMR (D$_2$O, 500MHz): δ 9.18 (br, 1H), 7.90 (m, 2H), 5.01 (s, 1H), 4.39 (t, J = 10.5 Hz, 1H), 4.19 (m, 1H), 4.11 (m, 2H), 4.03 (t, J = 10.0 Hz, 1H), 3.96 (t, J = 10.0 Hz, 1H), 3.77 (t, J = 10.0 Hz, 1H), 3.51 (dd, J = 11.3, 2.5 Hz, 1H), 3.41 (t, J =9.5 Hz, 1H), 3.25 (dd, J = 10.3, 3.0 Hz, 1H), 3.22 (dd, J = 10.75, 2.5 Hz, 1H), 2.82 (s, 3H), 2.81 (s, 3H), 1.92-1.86 (m, 1H), 1.78-1.75 (m, 1H), 1.25 (d, J = 5.5 Hz, 3H). HRMS-ESI calcd for $C_{20}H_{32}N_5O_7$ [M+H]$^+$ 454.2302, found: 454.2300.

3'-Dihydro-3'-deoxy-3'(R)- (pyrazin-2-yl)acetylamino spectinomycin trihydrobromide (15):

Method 2, Yield: 64%. ^{1}H NMR (400 MHz, D$_2$O) δ 8.58 (m, 3H), 5.02 (s, 1H), 4.40 (dd, J = 9.7, 11.1 Hz, 1H), 4.19 (t, J = 3.2 Hz, 1H), 4.11 − 3.95 (m, 5H), 3.52 (dd, J = 2.8, 11.1 Hz, 1H), 3.27 (dd, J = 2.9, 10.1 Hz, 1H), 2.83 (s, 3H), 2.82 (s, 3H), 1.93 − 1.87 (m, 1H), 1.81 − 1.74 (m, 1H), 1.26 (d, J = 6.1 Hz, 3H). HRMS-ESI calcd for C$_{20}$H$_{32}$N$_5$O$_7$ [M+H]$^+$ 454.2302, found: 454.2290.

3'-Dihydro-3'-deoxy-3'(R)- (pyrimidin-4-yl)acetylamino spectinomycin trihydrobromide

(16): Method 2, Yield: 59%. ^{1}H NMR (400 MHz, Deuterium Oxide) δ 9.13 (d, J = 1.3 Hz, 1H), 8.80 (d, J = 5.4 Hz, 1H), 7.64 (dd, J = 1.4, 5.4 Hz, 1H), 5.01 (s, 1H), 4.40 (dd, J = 9.7, 11.1 Hz, 1H), 4.23 − 4.18 (m, 1H), 4.14 − 3.92 (m, 3H), 3.53 (dd, J = 2.8, 11.1 Hz, 1H), 3.27 (dd, J = 2.9, 10.1 Hz, 1H), 2.83 (d, J = 1.1 Hz, 7H), 1.91 (ddd, J = 3.9, 10.0, 14.9 Hz, 1H), 1.78 (d, J = 14.5 Hz, 1H), 1.26 (d, J = 6.1 Hz, 3H). MS-ESI: m/z 454 (M$^+$+H).

3'-Dihydro-3'-deoxy-3'(R)-(2-aminothiazol-4-yl)acetylamino spectinomycin

trihydrobromide (18): Method 2, Yield: 67%. ^{1}H NMR (D$_2$O, 500MHz): δ 6.61 (s, 1H), 4.98 (s, 1H), 4.39 (t, J = 10.0 Hz, 1H), 4.18 (t, J = 3.0 Hz, 1H), 4.05-3.94 (m, 3H), 3.77 (m, 1H), 3.71 (d, J = 6.5 Hz, 1H), 3.63 (q, J = 7.0 Hz, 1H), 3.51 (dd, J = 11.0, 2.5 Hz, 1H), 3.22 (dd, J = 10.5, 2.5 Hz, 1H), 2.83 (s, 3H), 2.82 (s, 3H), 1.93-1.87 (m, 1H), 1.77-1.74 (m, 1H), 1.25 (d, J = 6.0 Hz, 3H). HRMS-ESI calcd for C$_{19}$H$_{32}$N$_5$O$_7$S [M+H]$^+$ 474.2022, found: 474.2011.

3'-Dihydro-3'-deoxy-3'(R)-(thiazol-2-yl) acetylamino spectinomycin trihydrobromide (19):

Method 2, Yield: 60%. ^{1}H NMR (400 MHz, D$_2$O): δ 7.88 (d, J = 3.6 Hz, 1H), 7.74 − 7.65 (m, 1H), 4.98 (s, 1H), 4.74 (t, J =2.7 Hz, 1H), 4.37 (dd, J = 11.0, 9.9 Hz, 1H), 4.17 (t, J = 3.1 Hz, 1H), 4.10 − 3.89 (m, 4H), 3.52 − 3.47 (m, 1H), 3.24 (dd, J = 10.1, 2.9 Hz, 1H), 2.81 (s, 6H), 1.94 − 1.82 (m, 1H), 1.79 − 1.71 (m, 1H), 1.23 (d, J = 6.1 Hz, 3H). HRMS-ESI calcd for C$_{19}$H$_{31}$N$_4$O$_7$S [M+H]$^+$ 459.1913, found: 459.1909.

3'-Dihydro-3'-deoxy-3'(R)-(1*H*-imidazol-4-yl)acetylamino spectinomycin trihydrobromide

(20): Method 2, Yield: 65%. ^{1}H NMR (400 MHz, D2O): δ 8.67 (d, *J* = 1.4 Hz, 1H), 7.36 (d, *J* = 1.3 Hz, 1H), 5.00 (s, 1H), 4.90 (s, 1H), 4.40 (dd, *J* = 10.9, 10.0 Hz, 1H), 4.19 (t, *J* = 3.0 Hz, 1H), 4.13 – 3.90 (m, 3H), 3.88 (d, *J* = 3.5 Hz, 2H), 3.54 (dd, *J* = 7.9, 3.3 Hz, 1H), 3.27 (dd, *J* = 10.2, 2.7 Hz, 1H), 2.83 (s, 6H), 1.96 – 1.85 (m, 1H), 1.76 (dd, *J* = 12.3, 2.3 Hz, 1H), 1.26 (d, *J* = 6.1 Hz, 3H). HRMS-ESI calcd for $C_{19}H_{32}N_5O_7$ $[M+H]^+$ 442.2302, found: 442.2908.

3'-Dihydro-3'-deoxy-3'(R)-(1*H*-imidazol-2-yl)acetylamino spectinomycin trihydrochloride

(21): Method 1, Yield: 64%. ^{1}H NMR (400 MHz, Deuterium Oxide) δ 7.35 (s, 2H), 4.93 (s, 1H), 4.33 (dd, *J* = 9.8, 11.1 Hz, 1H), 4.12 (t, *J* = 3.3 Hz, 3H), 4.09 – 3.85 (m, 3H), 3.52 – 3.42 (m, 1H), 3.20 (dd, *J* = 2.9, 10.2 Hz, 1H), 2.77 (s, 6H), 1.84 (ddd, *J* = 4.0, 11.8, 15.3 Hz, 1H), 1.75 – 1.67 (m, 1H), 1.20 (d, *J* = 6.1 Hz, 3H). MS-ESI: m/z 442 (M^++H).

3'-Dihydro-3'-deoxy-3'(R)-(1*H*-pyrazol-1-yl)acetylamino spectinomycin trihydrobroride

(22): Method 2, Yield: 69%. ^{1}H NMR (400 MHz, Deuterium Oxide) δ 7.65 (dd, *J* = 0.7, 2.5 Hz, 1H), 7.60 (dd, *J* = 0.7, 2.0 Hz, 1H), 6.37 (t, *J* = 2.3 Hz, 1H), 4.97 (d, *J* = 2.0 Hz, 2H), 4.89 (s, 1H), 4.31 (dd, *J* = 9.7, 11.1 Hz, 1H), 4.10 (t, *J* = 3.2 Hz, 1H), 4.01 – 3.84 (m, 3H), 3.45 (dd, *J* = 2.7, 11.1 Hz, 1H), 3.24 – 3.15 (m, 1H), 2.75 (d, *J* = 2.2 Hz, 6H), 1.81 (ddd, *J* = 3.9, 11.6, 15.2 Hz, 1H), 1.71 (dt, *J* = 2.5, 14.4 Hz, 1H), 1.18 (d, *J* = 6.2 Hz, 3H). MS-ESI: m/z 442 (M^++H).

3'-Dihydro-3'-deoxy-3'(R)- (1*H*-imidazol-1-yl)acetylamino spectinomycin trihydrobromide

(23) Method 2, Yield: 77%. ^{1}H NMR (400 MHz, D_2O) δ 8.80 (t, *J* = 1.50 Hz, 1H), 7.52 (t, *J* = 1.75 Hz, 1H), 7.49 (t, *J* = 1.80 Hz, 1H), 5.17 (d, *J* = 3.18 Hz, 2H), 5.00 (s, 1H), 4.76 (t, *J* = 2.86 Hz, 1H), 4.39 (dd, *J* = 9.80, 11.12 Hz, 1H), 4.21 (dd, *J* = 2.62, 3.75 Hz, 1H), 4.10 – 3.94 (m, 3H), 3.57 – 3.51 (m, 1H), 3.31 – 3.24 (m, 1H), 2.83 (s, 6H), 1.92 (ddd, *J* = 3.99, 11.75, 15.30 Hz,

1H), 1.81 – 1.75 (m, 1H), 1.26 (d, J = 6.13 Hz, 3H). HRMS-ESI calcd for $C_{19}H_{32}N_5O_7$ [M+H]$^+$

442.2302, found: 442.2316.

3'-Dihydro-3'-deoxy-3'(R)-(benzo[*d*]oxazol-2-yl)acetylamino spectinomycin

trihydrobroride (24): Method 2, Yield: 62%. ^{1}H NMR (400 MHz, D$_2$O) δ 7.73 (dd, J = 6.5, 2.5

Hz, 1H), 7.67 (dd, J = 6.8, 2.4 Hz, 1H), 7.50 – 7.42 (m, 2H), 5.02 (s, 1H), 4.90 (s, 1H), 4.44 –

4.37 (m, 1H), 4.22 (t, J = 3.0 Hz, 1H), 4.12 – 3.95 (m, 3H), 3.53 (dd, J = 11.1, 2.6 Hz, 1H), 3.27

(dd, J = 10.1, 2.7 Hz, 1H), 2.83 (s, 8H), 1.97 – 1.86 (m, 1H), 1.82 (d, J = 14.4 Hz, 1H), 1.27 (d, J

= 6.1 Hz, 3H). HRMS-ESI calcd for $C_{23}H_{33}N_4O_8$ [M+H]$^+$ 493.2298, found: 493.2287.

3'-Dihydro-3'-deoxy-3'(R)-(benzo[*d*]thiazol-2-yl)acetylamino spectinomycin

trihydrobroride (25): Method 2, Yield: 73%. ^{1}H NMR (400 MHz, D$_2$O) δ 8.03 (dd, J = 17.1,

8.1, 2H), 7.65 – 7.57 (m, 1H), 7.57 – 7.48 (m, 1H), 5.03 (s, 1H), 4.77 (t, J = 2.7, 1H), 4.44 – 4.37

(m, 1H), 4.23 (t, J = 3.1, 1H), 4.16 – 3.89 (m, 4H), 3.53 (dd, J = 8.3, 2.8, 1H), 3.27 (dd, J = 10.1,

2.8, 1H), 2.83 (d, J = 5.2, 6H), 1.97 – 1.85 (m, 1H), 1.80 (dd, J = 12.2, 2.3, 1H), 1.26 (d, J = 6.1,

3H). HRMS-ESI calcd for $C_{23}H_{33}N_4O_7S$ [M+H]$^+$ 509.2070, found: 509.2067.

3'-Dihydro-3'-deoxy-3'(R)-(1-methyl-1*H*-benzo[*d*]imidazol-2-yl)acetylamino

spectinomycin trihydrobroride (26): Method 2, Yield: 75%. ^{1}H NMR (400 MHz, D$_2$O) δ 7.83

(tt, J = 10.1, 3.6 Hz, 2H), 7.70 – 7.63 (m, 2H), 5.05 (s, 1H), 4.78 – 4.76 (m, 1H), 4.44 – 4.38 (m,

1H), 4.25 (t, J = 3.1 Hz, 1H), 4.19 – 3.95 (m, 7H), 3.55 (dd, J = 11.1, 2.7 Hz, 1H), 3.29 (dd, J =

10.2, 2.8 Hz, 1H), 2.85 (s, 3H), 2.84 (s, 3H), 2.01 – 1.91 (m, 1H), 1.82 (d, J = 14.6 Hz, 1H), 1.30

(d, J = 6.1 Hz, 3H). HRMS-ESI calcd for $C_{24}H_{36}N_5O_7$ [M+H]$^+$ 506.2615, found: 506.2607.

3'-Dihydro-3'-deoxy-3'(R)-(1*H*-benzo[*d*]imidazol-2-yl)acetylamino spectinomycin

trihydrobroride (27): Method 2, Yield: 75%. ^{1}H NMR (400 MHz, D$_2$O) δ 7.84 – 7.78 (m, 2H),

7.65 – 7.59 (m, 2H), 5.03 (s, 1H), 4.45 – 4.36 (m, 1H), 4.24 (t, J = 3.1 Hz, 1H), 4.17 – 3.94 (m,

3H), 3.56 (dd, J = 11.1, 2.7 Hz, 1H), 3.29 (dd, J = 10.2, 2.8 Hz, 1H), 2.84 (s, 6H), 1.99 – 1.89

(m, 1H), 1.88 – 1.78 (m, 1H), 1.28 (d, J = 6.1 Hz, 3H). HRMS-ESI calcd for $C_{23}H_{34}N_5O_7$

$[M+H]^+$ 492.2458, found: 492.2458.

3'-Dihydro-3'-deoxy-3'(R)-(1*H*-indol-2-yl)acetylamino spectinomycin (28): Method 1, only

methanol as solvent, Yield: 75%. ^{1}H NMR (400 MHz, D_2O) δ 7.62 – 7.38 (m, 2H), 7.28 – 6.97

(m, 2H), 6.36 (d, J = 0.9 Hz, 1H), 4.86 (s, 1H), 4.26 (t, J = 10.5 Hz, 1H), 4.18 – 4.05 (m, 1H),

3.98 – 3.74 (m, 5H), 3.27 (s, 1H), 3.09 (d, J = 10.1 Hz, 1H), 2.73 – 2.59 (m, 6H), 1.86 – 1.76 (m,

1H), 1.76 – 1.63 (m, 1H), 1.18 (dd, J = 6.1, 24.6 Hz, 3H). HRMS-ESI calcd for $C_{24}H_{35}N_4O_7$

$[M+H]^+$ 491.2506, found: 491.2504.

3'-Dihydro-3'-deoxy-3'(R)- (3-methylpyridin-2-yl)acetylamino spectinomycin

trihydrobromide (29): Method 2, Yield: 78%. ^{1}H NMR (400 MHz, D_2O) δ 8.57 (d, J = 5.8 Hz,

1H), 8.41 (d, J = 7.9 Hz, 1H), 7.89 (dd, J = 5.9, 8.0 Hz, 1H), 5.03 (s, 1H), 4.39 (dd, J =9.8, 11.1

Hz, 1H), 4.24 – 4.16 (m, 2H), 4.15 – 3.93 (m, 3H), 3.55 – 3.50 (m, 1H), 3.27 (dd, J =2.9, 10.2

Hz, 1H), 2.82 (s, *3*H), 2.81 (s, *3*H), 1.98 – 1.88 (m, 1H), 1.77 (d, J = 14.4 Hz, 1H), 1.27 (d, J =

6.1 Hz, 3H). HRMS-ESI calcd for $C_{22}H_{35}N_4O_7$ $[M+H]^+$ 467.2506, found: 467.2500.

3'-Dihydro-3'-deoxy-3'(R)- (4-methylpyridin-2-yl)acetylamino spectinomycin

trihydrobromide (30): Method 2, Yield: 66%. ^{1}H NMR (400 MHz, D_2O) δ 8.56 (d, J = 6.2 Hz,

1H), 7.81 (d, J = 6.1 Hz, 1H), 7.78 (s, 1H), 5.03 (s, 1H), 4.44 – 4.37 (m, 1H), 4.21 (s, 1H), 4.18 –

3.95 (m, 5H), 3.55 (dd, J = 11.1, 2.6 Hz, 1H), 3.28 (dd, J = 10.1, 2.7 Hz, 1H), 2.85 (s, 6H), 2.65

(s, 3H), 1.98 – 1.87 (m, 1H), 1.78 (d, J = 14.7 Hz, 1H), 1.28 (d, J = 6.1 Hz, 3H). HRMS-ESI

calcd for $C_{22}H_{35}N_4O_7$ $[M+H]^+$ 467.2506, found: 467.2508.

3'-Dihydro-3'-deoxy-3'(R)- (5-methylpyridin-2-yl)acetylamino spectinomycin

trihydrobromide (31): Method 2, Yield: 66%. ^{1}H NMR (400 MHz, D_2O) δ 8.59 (s, 1H), 8.40 (d,

J = 7.6 Hz, 1H), 7.84 (d, *J* = 8.2 Hz, 1H), 5.03 (s, 1H), 4.44 – 4.37 (m, 1H), 4.20 (dd, *J* = 14.8,

6.0 Hz, 3H), 4.13 – 3.94 (m, 3H), 3.55 (dd, *J* = 11.2, 2.6 Hz, 1H), 3.29 (dd, *J* = 10.2, 2.6 Hz,

1H), 2.85 (s, 6H), 2.54 (s, 3H), 1.99 – 1.88 (m, 1H), 1.78 (d, *J* = 14.7 Hz, 1H), 1.28 (d, *J* = 6.1

Hz, 3H). HRMS-ESI calcd for $C_{22}H_{35}N_4O_7$ [M+H]$^+$ 467.2506, found: 467.2510.

3'-Dihydro-3'-deoxy-3'(R)- (6-methylpyridin-2-yl)acetylamino spectinomycin

trihydrobromide (32): Method 2, Yield: 85%. ^{1}H NMR (400 MHz, D$_2$O) δ 8.39 (t, *J* = 8.0 Hz,

1H), 7.79 (d, *J* = 8.1 Hz, 1H), 7.73 (d, *J* = 7.9 Hz, 1H), 5.03 (s, 1H), 4.77 (t, *J* = 2.8 Hz, 1H),

4.44 – 4.37 (m, 1H), 4.21 (dd, *J* = 5.7, 2.5 Hz, 1H), 4.18 – 3.94 (m, 5H), 3.55 (dd, *J* = 11.1, 2.7

Hz, 1H), 3.28 (dd, *J* = 10.2, 2.8 Hz, 1H), 2.84 (s, 3H), 2.83 (s, 3H), 2.79 (s, 3H), 1.92 (ddd, *J* =

15.4, 11.9, 3.9 Hz, 1H), 1.78 (d, *J* = 14.5 Hz, 1H), 1.28 (d, *J* = 6.1 Hz, 3H). HRMS-ESI calcd for

$C_{22}H_{35}N_4O_7$ [M+H]$^+$ 467.2506, found: 467.2521.

3'-Dihydro-3'-deoxy-3'(R)- (4-isopropylpyridin-2-yl)acetylamino spectinomycin

trihydrobromide (33): Method 2, Yield: 52%. ^{1}H NMR (400 MHz, D$_2$O) δ 8.58 (d, *J* = 6.2 Hz,

1H), 7.86 (dd, *J* = 1.9, 6.20 Hz, 1H), 7.83 (d, *J* = 1.7 Hz, 1H), 5.02 (s, 1H), 4.45 – 4.35 (m, 1H),

4.23 – 4.18 (m, 1H), 4.18 – 3.93 (m, 5H), 3.54 (dd, *J* = 2.8, 11.02 Hz, 1H), 3.31 – 3.25 (m, 1H),

3.24 – 3.16 (m, 1H), 2.83 (s, 3H), 2.82 (s, 3H), 1.99 – 1.86 (m, 1H), 1.77 (dt, *J* = 2.4, 14.5 Hz,

1H), 1.32 (d, *J* = 6.9 Hz, 6H), 1.27 (d, *J* = 6.2 Hz, 3H). HRMS-ESI calcd for $C_{24}H_{39}N_4O_7$

[M+H]$^+$ 439.2193, found: 439.2188.

3'-Dihydro-3'-deoxy-3'(R)- (4-methoxypyridin-2-yl)acetylamino spectinomycin

trihydrobromide (34): Method 2, Yield: 48%. ^{1}H NMR (400 MHz, D$_2$O) δ 8.51 (d, *J* = 7.0 Hz,

1H), 7.41 (dd, *J* = 6.9, 2.7 Hz, 1H), 7.37 (d, *J* = 2.7 Hz, 1H), 5.02 (s, 1H), 4.45 – 4.36 (m, 1H),

4.21 (s, 1H), 4.14 – 3.94 (m, 8H), 3.54 (dd, *J* = 11.1, 2.7 Hz, 1H), 3.28 (dd, *J* = 10.2, 2.7 Hz,

1H), 2.84 (s, 6H), 1.96 – 1.87 (m, 1H), 1.83 – 1.72 (m, 1H), 1.28 (d, J = 6.1 Hz, 3H). HRMS-ESI

calcd for $C_{22}H_{35}N_4O_8$ [M+H]$^+$ 483.2455, found: 483.2435.

3'-Dihydro-3'-deoxy-3'(R)- (4-hydroxypyridin-2-yl)acetylamino spectinomycin

trihydrochloride (35): Method 1, Yield: 86%. ^{1}H NMR (400 MHz, D$_2$O) δ 7.88 (d, J = 7.2 Hz,

1H), 6.55 (dd, J = 2.5, 7.2 Hz, 1H), 6.50 (d, J = 2.6 Hz, 1H), 4.95 (s, 1H), 4.48 (t, J = 2.9 Hz,

1H), 4.17 – 4.15 (m, 1H), 4.05 (dd, J = 6.7, 11.6 Hz, 1H), 3.95 (t, J = 9.9 Hz, 1H), 3.80 – 3.70

(m, 2H), 2.86 (dd, J = 2.71, 10.9 Hz, 1H), 2.76 (dd, J = 2.9, 10.41 Hz, 1H), 2.56 (s, 3H), 2.48 (s,

3H), 1.92 (ddd, J = 3.9, 11.7, 15.1 Hz, 1H), 1.76 (dt, J = 2.4, 14.4 Hz, 1H), 1.27 (d, J = 6.1 Hz,

3H). HRMS-ESI calcd for $C_{21}H_{33}N_4O_8$ [M+H]$^+$ 469.2298, found: 469.2295.

3'-Dihydro-3'-deoxy-3'(R)- (5-aminopyridin-2-yl)acetylamino spectinomycin

trihydrobromide (37): Method 2, Yield: 65%. ^{1}H NMR (400 MHz, D$_2$O) δ 7.94 (d, J = 2.7 Hz,

1H), 7.67 (dd, J = 2.8, 8.8 Hz, 1H), 7.49 (d, J = 8.8 Hz, 1H), 4.92 (s, 1H), 4.30 (dd, J = 9.7, 11.1

Hz, 1H), 4.09 (t, J = 3.2 Hz, 1H), 4.02 – 3.84 (m, 5H), 3.44 (dd, J = 3.3, 7.96 Hz, 1H), 3.18 (dd,

J = 2.9, 10.2 Hz, 1H), 2.74 (s, 3H), 2.73 (s, 3H), 1.82 (ddd, J = 3.9, 11.8, 15.3 Hz, 1H), 1.67 (dt,

J = 2.3, 14.5 Hz, 1H), 1.17 (d, J = 6.1 Hz, 3H). HRMS-ESI calcd for $C_{21}H_{34}N_5O_7$ [M+H]$^+$

468.2458, found: 468.2457.

3'-Dihydro-3'-deoxy-3'(R)- (5-methoxypyridin-2-yl)acetylamino spectinomycin

trihydrobromide (38): Method 2, Yield: 60%. ^{1}H NMR (400 MHz, D$_2$O) δ 8.42 (d, J = 2.9 Hz,

1H), 8.07 (dd, J = 9.0, 2.9 Hz, 1H), 7.81 (d, J = 9.0 Hz, 1H), 5.02 (s, 1H), 4.44 – 4.36 (m, 1H),

4.20 (s, 1H), 4.13 – 3.94 (m, 8H), 3.58 – 3.51 (m, 1H), 3.28 (dd, J = 10.1, 2.8 Hz, 1H), 2.84 (s,

3H), 2.83 (s, 3H), 1.99 – 1.87 (m, 1H), 1.78 (d, J = 14.7 Hz, 1H), 1.28 (d, J = 6.1 Hz, 3H).

HRMS-ESI calcd for $C_{22}H_{35}N_4O_8$ [M+H]$^+$ 483.2455, found: 483.2459.

3'-Dihydro-3'-deoxy-3'(R)- (5-hydroxypyridin-2-yl)acetylamino spectinomycin

trihydrochloride (39): Method 1, Yield: 90%. ^{1}H NMR (400 MHz, D$_2$O) δ 8.04 (dd, J = 0.8, 2.9

Hz, 1H), 7.34 – 7.25 (m, 2H), 4.97 (s, 1H), 4.59 (t, J = 2.9 Hz, 1H), 4.32 – 4.22 (m, 1H), 4.16 (t,

J = 3.2 Hz, 1H), 4.11 – 3.73 (m, 5H), 3.14 (dd, J = 2.7, 10.9 Hz, 1H), 3.01 (dd, J = 2.8, 10.3 Hz,

1H), 2.70 (s, 3H), 2.62 (s, 3H), 1.93 – 1.85 (m, 1H), 1.77 (dt, J = 2.4, 14.3 Hz, 1H), 1.26 (d, J =

6.08 Hz, 3H). HRMS-ESI calcd for C$_{21}$H$_{33}$N$_4$O$_8$ [M+H]$^+$ 469.2298, found: 469.2301.

3'-Dihydro-3'-deoxy-3'(R)- (5-(difluoromethoxy)pyridin-2-yl)acetylamino spectinomycin

trihydrochloride (40): Method 1, Yield: 83%. ^{1}H NMR (400 MHz, D$_2$O) δ 8.40 (d, J = 2.8 Hz,

1H), 7.71 (dd, J = 2.8, 8.6 Hz, 1H), 7.46 (dd, J = 0.7, 8.6 Hz, 1H), 6.90 (t, J = 72.9 Hz, 1H), 5.00

(s, 1H), 4.66 (t, J = 2.8 Hz, 1H), 4.32 (dd, J = 9.9, 11.1 Hz, 1H), 4.18 (t, J = 3.2 Hz, 1H), 4.09

(dtd, J = 1.9, 6.3, 11.8 Hz, 1H), 4.01 (t, J = 9.9 Hz, 1H), 3.94 – 3.86 (m, 3H), 3.32 – 3.26 (m,

1H), 3.11 (dd, J = 2.8, 10.3 Hz, 1H), 2.76 (s, 3H), 2.70 (s, 3H), 1.91 (ddd, J = 3.9, 11.6, 15.3 Hz,

1H), 1.78 (dt, J = 2.4, 14.5 Hz, 1H), 1.27 (d, J = 6.1 Hz, 3H). HRMS-ESI calcd for

C$_{22}$H$_{33}$F$_2$N$_4$O$_8$ [M+H]$^+$ 519.2266, found: 519.2271.

3'-Dihydro-3'-deoxy-3'(R)- (5-(trifluoromethoxy)pyridin-2-yl)acetylamino spectinomycin

trihydrochloride (41): Method 1, Yield: 88%. ^{1}H NMR (400 MHz, D$_2$O) δ 8.54 – 8.50 (m, 1H),

7.87 – 7.82 (m, 1H), 7.51 (d, J = 8.6 Hz, 1H), 5.00 (s, 1H), 4.66 (t, J = 2.8 Hz, 1H), 4.36 – 4.29

(m, 1H), 4.19 (t, J = 3.2 Hz, 1H), 4.08 (ddd, J = 2.0, 6.14, 11.8 Hz, 1H), 4.01 (t, J = 9.9 Hz, 1H),

3.96 – 3.86 (m, 3H), 3.29 (d, J = 11.0 Hz, 1H), 3.12 (dd, J = 2.8, 10.17 Hz, 1H), 2.76 (s, 3H),

2.71 (s, 3H), 1.91 (ddd, J = 3.98, 11.6, 15.1 Hz, 1H), 1.78 (dt, J = 2.4, 14.4 Hz, 1H), 1.27 (d, J =

6.1 Hz, 3H). HRMS-ESI calcd for C$_{22}$H$_{32}$F$_3$N$_4$O$_8$ [M+H]$^+$ 537.2172, found: 537.2161.

3'-Dihydro-3'-deoxy-3'(R)-(5-bromopyridin-2-yl)acetylamino spectinomycin

trihydrobromide   (43): Method 2, Yield: 60%. ^{1}H NMR (400 MHz, D2O): δ 8.77 (s, 1H),

8.33 (s, 1H), 7.58 (s, 1H), 5.03 (s, 1H), 4.78 (s, 1H), 4.42 (dd, J = 10.9, 9.9 Hz, 1H), 4.20 (d, J = 3.0 Hz,1H), 4.14 – 3.95 (m, 5H), 3.55 (dd, J = 11.2, 2.5 Hz, 1H), 3.29 (dd, J = 10.1, 2.7 Hz, 1H), 2.85 (s, 3H), 2.84 (s, 3H), 1.96 – 1.88 (m, 1H), 1.79 (d, J = 14.6 Hz, 1H), 1.28 (d, J = 6.1 Hz, 3H). HRMS-ESI calcd for $C_{21}H_{32}BrN_4O_7$ [M+H]$^+$ 531.1454, found: 531.1469.

3'-Dihydro-3'-deoxy-3'(R)- (4-chloro-3-isopropylpyridin-2-yl)acetylamino spectinomycin trihydrobromide (45): Method 2, Yield: 68%. ^{1}H NMR (400 MHz, D$_2$O) δ 8.51 (d, J = 6.3 Hz, 1H), 8.01 (d, J = 6.3 Hz, 1H), 5.04 (s, 1H), 4.45 – 4.35 (m, 1H), 4.35 – 4.27 (m, 1H), 4.19 (t, J = 3.2 Hz, 1H), 4.16 – 3.91 (m, 3H), 3.56 – 3.52 (m, 1H), 3.27 (dd, J = 2.8, 10.2 Hz, 1H), 2.83 (s, 3H), 2.82 (s, 3H), 1.93 (ddd, J = 3.9, 11.8, 15.3 Hz, 1H), 1.79 – 1.71 (m, 1H), 1.41 (t, J = 7.1 Hz, 6H), 1.28 (d, J = 6.2 Hz, 3H). HRMS-ESI calcd for $C_{24}H_{38}ClN_4O_7$ [M+H]$^+$ 529.2429, found: 529.2432.

3'-Dihydro-3'-deoxy-3'(R)- (4-chloro-3-methylpyridin-2-yl)acetylamino spectinomycin trihydrobromide (46): Method 2, Yield: 66%. ^{1}H NMR (400 MHz, D$_2$O) δ 8.43 (d, J = 6.3 Hz, 1H), 7.92 (d, J = 6.3 Hz, 1H), 4.94 (s, 1H), 4.67 (t, J = 2.9 Hz, 1H), 4.34 – 4.27 (m, 1H), 4.11 (t, J = 3.1 Hz, 1H), 4.08 – 3.83 (m, 4H), 3.45 (dd, J = 11.1, 2.7 Hz, 1H), 3.18 (dd, J = 10.2, 2.8 Hz, 1H), 2.74 (s, 3H), 2.73 (s, 3H), 2.40 (s, 3H), 1.88 – 1.79 (m, 1H), 1.73 – 1.65 (m, 1H), 1.19 (d, J = 6.1 Hz, 3H). HRMS-ESI calcd for $C_{22}H_{34}ClN_4O_7$ [M+H]$^+$ 501.2116, found: 501.2120.

3'-Dihydro-3'-deoxy-3'(R)- (4-chloro-5-methylpyridin-2-yl)acetylamino spectinomycin trihydrobromide (47): Method 2, Yield: 81%. ^{1}H NMR (400 MHz, D$_2$O) δ 8.64 (s, 1H), 7.98 (s, 1H), 5.02 (s, 1H), 4.78 – 4.76 (m, 1H), 4.43 – 4.37 (m, 1H), 4.20 (t, J = 3.1 Hz, 1H), 4.16 – 3.94 (m, 5H), 3.58 – 3.52 (m, 1H), 3.28 (dd, J = 10.2, 2.7 Hz, 1H), 2.84 (s, 3H), 2.83 (s, 3H), 2.52 (s, 3H), 1.97 – 1.88 (m, 1H), 1.78 (d, J = 14.5 Hz, 1H), 1.27 (d, J = 6.2 Hz, 3H). HRMS-ESI calcd for $C_{22}H_{34}ClN_4O_7$ [M+H]$^+$ 501.2116, found: 501.2116.

3'-Dihydro-3'-deoxy-3'(R)- (4-chloro-5-methoxypyridin-2-yl)acetylamino spectinomycin trihydrobromide (48): Method 2, Yield: 98%.^{1}H NMR (400 MHz, D$_2$O) δ 8.44 (s, 1H), 7.87 (s, 1H), 5.01 (s, 1H), 4.40 (dd, J = 9.8, 11.1 Hz, 1H), 4.19 (t, J = 3.3 Hz, 1H), 4.14 – 3.93 (m, 5H), 4.08 (s, 3H), 3.53 (dd, J = 2.8, 11.1 Hz, 1H), 3.27 (dd, J = 2.9, 10.1 Hz, 1H), 2.83 (s, 3H), 2.82 (s, 3H), 1.95 – 1.87 (m, 1H), 1.77 (dt, J = 2.4, 14.47 Hz, 1H), 1.27 (d, J = 6.2 Hz, 3H). HRMS-ESI calcd for C$_{22}$H$_{34}$ClN$_4$O$_8$ [M+H]$^+$ 517.2065, found: 517.2061.

3'-Dihydro-3'-deoxy-3'(R)- (4-chloro-5-fluoropyridin-2-yl)acetylamino spectinomycin trihydrobromide (49): Method 2, Yield: 69%. ^{1}H NMR (400 MHz, D$_2$O) δ 8.54 (d, J = 1.8 Hz, 1H), 7.71 (d, J = 5.9 Hz, 1H), 5.00 (s, 1H), 4.76 (t, J = 2.9 Hz, 1H), 4.39 (dd, J = 9.7, 11.1 Hz, 1H), 4.18 (t, J = 3.3 Hz, 1H), 4.11 – 3.92 (m, 5H), 3.52 (dd, J = 2.7, 11.1 Hz, 1H), 3.26 (dd, J = 2.9, 10.1 Hz, 1H), 2.82 (s, 3H), 2.81 (s, 3H), 1.89 (ddd, J = 4.0, 11.7, 15.3 Hz, 1H), 1.76 (dt, J = 2.4, 14.4 Hz, 1H), 1.25 (d, J = 6.1 Hz, 3H). HRMS-ESI calcd for C$_{21}$H$_{31}$ClFN$_4$O$_7$ [M+H]$^+$ 505.1865, found: 505.1866.

3'-Dihydro-3'-deoxy-3'(R)- (5-fluoro-4-methoxypyridin-2-yl)acetylamino spectinomycin trihydrochloride (50): Method 1, Yield: 88%. ^{1}H NMR (400 MHz, D$_2$O) δ 8.60 (d, J = 4.6 Hz, 1H), 7.57 (d, J = 7.3 Hz, 1H), 5.03 (s, 1H), 4.41 (dd, J = 11.1, 9.7 Hz, 1H), 4.21 (t, J = 3.3 Hz, 1H), 4.18 (s, 3H), 4.11 (d, J = 5.9 Hz, 2H), 4.07 – 3.94 (m, 2H), 3.55 (dd, J = 11.1, 2.7 Hz, 1H), 3.29 (dd, J = 10.2, 2.8 Hz, 1H), 2.85 (s, 3H), 2.84 (s, 3H), 1.93 (ddd, J = 15.4, 11.8, 4.0 Hz, 1H), 1.79 (dt, J = 14.4, 2.3 Hz, 1H), 1.28 (d, J = 6.1 Hz, 3H). HRMS-ESI calcd for C$_{22}$H$_{34}$FN$_4$O$_8$ [M+H]$^+$ 501.2361, found: 501.2356.

Crystal structure determination

1 tri hydrobromide salt was crystalized from methanol-acetone. A colorless, plate-like specimen

of approximate dimensions 0.45 mm x 0.40 mm x 0.15 mm was cleaved from a larger crystal.

The selected crystal (colorless, 0.45 mm x 0.40 mm x 0.15 mm) was affixed to a nylon sample

support via silicone grease, and flash cooled to 100K for x-ray analysis on a Bruker D8 3-circle

diffractometer with fixed χ. The crystal was illuminated with the X-ray beam from a FR-591

rotating-anode X-ray generator equipped with a copper anode and Helios focusing mirrors. The

resulting images were integrated with the Bruker SAINT software package using a narrow-frame

algorithm. Integration of the data based on a monoclinic unit cell yielded a total of 45050

reflections to a maximum θ angle of 71.58° (0.81 Å resolution), of which 5547 were independent

and 5538 (99.8%) were considered observed. The data were substantially complete (97.7%) to a

θ angle of 67.75° (0.83 Å). A multiscan absorption correction was applied, and data were

corrected for inter-frame scaling differences, via program SADABS.The structure was solved

and refined via the Bruker SHELXTL software package, using the space group $P2_1$, with $Z = 2$

for the formula unit, $C_{21}H_{41.6}Br_3N_4O_{10.3}$. Hydrogen atoms were located in difference electron

density maps but refined according to a riding model. The final anisotropic full-matrix least-

squares refinement converged at $R1 = 2.90\%$ for the observed data and $wR2 = 7.60\%$ for all data.

The largest peak in the final difference electron density synthesis was 1.254 e−/Å^3, at a position

near one of the bromine atoms, and the deepest hole was −0.869 e−/Å^3, with an RMS deviation

of 0.086 e−/Å^3.

Molecular modeling.

A homology model for *M. tuberculosis* ribosome was built from the crystal structure of

Escherichia coli ribosome in complex with spectinomycin.[6] Within a 15Å radius of the ligand

center, one mutation A1081G was noted among the ribonucleic acids and two mutations T23V,

I29R among the S5 protein. To reduce computational overhead, a ≈15Å truncated sphere

centered on the ligand was only considered for simulation. This included parts of helix 34 to

helix 37 and a loop of the S5 protein. Nine magnesium ions from the crystal structure were

preserved.

The spectinamide series was geometry optimized in Jaguar at the B3LYP/6-31G** level of

approximation and docked into the binding site using Glide's Standard Precision mode.[22]

All molecular dynamics calculations were carried in AMBER11[23] using the ff10 force field for

the RNA and protein and General Amber Force Field (GAFF)[24] for the ligand. The parameters

used for Mg^{2+} were obtained from Aaqvist et al.[25] The positively charged spectinamides were

assigned Restrained Electrostatic Potential (RESP) charges with the ANTECHAMBER module

of AMBER. The whole complex was solvated in an octahedron box of TIP3P water molecules

keeping a minimum of 10 Å distance between the edge of the box and the solute and neutralized

by adding sodium ions. Periodic boundary conditions, particle-mesh Ewald (PME) treatment of

the long-term electrostatics and SHAKE-enabled 2-fs time steps were employed. A two-stage

energy minimization was performed with solute first constrained and then released. The

minimized system was gradually heated from 0K to 300K over 60ps at constant volume followed

by a 50ps equilibration at constant pressure. An additional 0.5 ns simulation at 300K was

performed to further optimize the system. All production runs were performed with the NPT

ensemble for 20 ns. Terminal residues were harmonically restrained.

Molecular dynamics snapshots taken at 10 ps intervals from the last 2 ns production run and

stripped of all counter ions and water molecules were used as structural ensembles for free

energy calculation using MM-PBSA methods. The electrostatic contributions to solvation were

calculated by solving PB using modules implemented in AMBER. The non-polar contribution

(ΔG_{np}) was calculated using

$$\Delta G_{np} = \gamma SASA + b \qquad\qquad (1)$$

where SASA is the solvent-accessible surface area, γ is the surface tension parameter, set to

0.00542 kcal/mol.Å^2 and b is the parameterized value, set to -1.008 kcal/mol.

Ribosomal inhibition:

Purified 70S *M. smegmatis* bacterial ribosomes were used in translation reactions. Firefly

luciferase mRNA was produced *in vitro* using T7 RNA polymerase. Translation reactions were

carried out as previously described.[26] The IC_{50} values represent the drug concentration that

inhibits luciferase activity by 50%.

Bacterial culture and antibacterial susceptibility testing. *M. tuberculosis* strains $H_{37}Rv$,

$H_{37}Rv$ $\Delta1258c$ ($H_{37}Rv$ parental with gene encoding efflux pump Rv1258c deleted) and $H_{37}Rv$

$\Delta1258c$ pCRS4 (efflux pump KO $H_{37}Rv\Delta1258c$ with Rv1258c promoter and gene encoded on

plasmid pCRS4) were cultured in Middlebrook 7H9 broth supplemented with 10% albumin–

dextrose complex 0.05% (v/v) Tween 80, shaking at 37°C. MICs were determined using the

microbroth dilution method according to CLSI standards and were read by visual inspection.

Two-fold serial dilutions of antibiotic in 100 µL of 7H9 broth medium were first prepared in 96-

well round-bottomed microtitre plates (Nunc, USA). An equivalent volume (100 µL) of bacterial

broth containing ~10^5 bacterial cfu/mL was added to each well to give final concentrations of

drug starting at 200 mg/L. Plates were incubated aerobically at 37°C for 7 days, at which point

the MIC was recorded as the lowest concentration of compound or drug that prevented visible

growth. At least 3 biologically independent replicates were performed with each strain.

Post Antibiotic Effect (PAE). PAE was determined as described previously.[27] PAE was

calculated as the difference between the time required to reach 50% saturation at OD600 (1.1 ±

0.2) for the untreated and treated cultures. Each treatment was tested in at least two biologically

independent experiments.

Mammalian Cytotoxicity. The toxicity of compounds towards Vero cells (ATCC CCL-81) was

determined as described previously,[28] except that compounds were dissolved in 1% DMSO such

that the final concentration of DMSO in the assay was less than 0.05%. The concentration of

each treatment that produced a 50% reduction in viability compared to untreated control was

defined at the IC_{50}.

Microsomal stability. The stability of compounds to mouse and human liver microsomal

degradation was determined as described previously, [29] the rate of degradation was monitored by

LC-MS analysis using multiple sampled time points. Metabolic stability was evaluated via the

half-life from least-squares fit of the concentration remaining at the time points based on first-

order kinetics.

Plasma protein binding. The mouse plasma protein binding of compounds was determined by

rapid equilibrium dialysis assay and LC-MS quantification, using a dialysis membrane (MWCO

~8,000) as previously described.[29]

Ethics statement. All animal efficacy studies were performed at Colorado State University in

accordance with guidelines of the Colorado State University Institutional Animal Care and Use

Committee.

Maximum tolerated dose. Escalating single doses of spectinamides (typically at 30, 100, and

300 mg/kg or 100, 200, and 400 mg/kg of body weight) were administered by subcutaneous

injection to three C57BL/6 female mice per dose on three consecutive days. Mice were observed

10 minutes and 1- and 4 hours following drug administration and then twice daily for the

duration of the study (1 week).

In vivo **efficacy.** Efficacy was determined using a mouse model of acute tuberculosis infection as

described previously.[30] Female IFN-γ KO mice between 8-10 weeks of age (Jackson

Laboratories) were infected with a low dose aerosol (100 CFU per mouse) of *M. tuberculosis*

Erdman (TMC 107, ATCC 35801) using a GlasCol aerosol chamber. Exerimental compounds

and stretomycin were administed by subcutaneous injection, while isoniazid was adminstered by

oral gavage. Groups of 4-5 mice received treatments for 9 consequtive days. The day after the

last treatment, lungs were harvested and pulmonary bacterial load determined by homogenization

and plating dilutions of homogenate on non-selective 7H11 agar plates. After 21 days of

incubation, the number of colonies on each plate was counted and CFU were converted to

logarithms, which were then evaluated by a one-way analysis of variance (ANOVA) followed by

a multiple-comparison ANOVA between carrier and compound treated groups by a one-way

Tukey test.

ASSOCIATED CONTENT

Supporting Information

The X-ray data collection, Structure Solution, and Refinement for **1**. Calculated free energy of

binding. Maximum tolerated dose of 9 spectinamide lead compounds. Full testing results for

compounds in the acute GKO mouse infection model, as monitored by CFUs. Activity of

spectinamides against multiple isolates of MDR and XDR tuberculosis. This information is

available free of charge via the Internet at

https://na01.safelinks.protection.outlook.com/?url=http%3A%2F%2Fpubs.acs.org%2F&data=01

%7C01%7Crichard.lee%40stjude.org%7Cf72b86e752014bf14de808d3e660efcb%7C22340fa89

2264871b677d3b3e377af72%7C0&sdata=Wcn6l63je%2BU8NrWdkY7kueX1rOY4iBek4qbuVJ

eRg%2Fo%3D&reserved=0.

AUTHOR INFORMATION

Corresponding Author

Phone: 901-595-6617. Email: Richard.lee@stjude.org

Author Contributions

R.E.L. designed the compound series. J.L., R., S.L.W. and T.A.B performed the medicinal

chemistry. D.F.B., R.B.L., H.I.B., B.G., and J.A. performed MIC testing and microbiology

studies. Z.Z. and S.D. performed the molecular modeling experiments. T.J., D.S. and E.C.B.

designed and performed MIC testing and ribosome inhibition studies. M.S.S., G.T.R. and A.J.L.

designed and performed the *in vivo* efficacy trials. L.Y. performed *in vitro* ADME testing. J.B.

performed X-Ray study. All authors discussed and analyzed the data. J.L., R.E.L., R.B.L., D.F.B.

and B.M. wrote the manuscript.

ABBREVIATIONS

M., Mycobacterium; SAR, structure activity relationship; Cbz, carboxybenzyl; MIC, minimum

inhibitory concentration; EW, electron withdrawing; ED, electron donating; KO, knockout; PAE,

post antibiotic effect; BID, twice daily; MTD, maximum tolerated dose

REFERENCES

1.   Hoagland, D.; Zhao, Y.; Lee, R. E., Advances in Drug Discovery and Development for Pediatric Tuberculosis. *Mini Rev Med Chem* **2016,** *16* (6), 481-97. DOI: 10.2174/1389557515666150722101723.
2.   Hoagland, D. T.; Liu, J.; Lee, R. B.; Lee, R. E., New agents for the treatment of drug-resistant Mycobacterium tuberculosis. *Adv Drug Deliv Rev* **2016,** *102*, 55-72. DOI: 10.1016/j.addr.2016.04.026.
3.   Mdluli, K.; Kaneko, T.; Upton, A., The tuberculosis drug discovery and development pipeline and emerging drug targets. *Cold Spring Harb Perspect Med* **2015,** *5* (6). DOI: 10.1101/cshperspect.a021154.
4.   Lee, R. E.; Hurdle, J. G.; Liu, J.; Bruhn, D. F.; Matt, T.; Scherman, M. S.; Vaddady, P. K.; Zheng, Z.; Qi, J.; Akbergenov, R.; Das, S.; Madhura, D. B.; Rathi, C.; Trivedi, A.; Villellas, C.; Lee, R. B.; Rakesh; Waidyarachchi, S. L.; Sun, D.; McNeil, M. R.; Ainsa, J. A.; Boshoff, H. I.; Gonzalez-Juarrero, M.; Meibohm, B.; Bottger, E. C.; Lenaerts, A. J., Spectinamides: a new class of semisynthetic antituberculosis agents that overcome native drug efflux. *Nat Med* **2014,** *20* (2), 152-8. DOI: 10.1038/nm.3458.

5.   Carter, A. P.; Clemons, W. M.; Brodersen, D. E.; Morgan-Warren, R. J.; Wimberly, B. T.; Ramakrishnan, V., Functional insights from the structure of the 30S ribosomal subunit and its interactions with antibiotics. *Nature* **2000,** *407* (6802), 340-8. DOI: 10.1038/35030019.

6.   Borovinskaya, M. A.; Shoji, S.; Holton, J. M.; Fredrick, K.; Cate, J. H., A steric block in translation caused by the antibiotic spectinomycin. *ACS Chem Biol* **2007,** *2* (8), 545-52. DOI: 10.1021/cb700100n.

7.   Balganesh, M.; Dinesh, N.; Sharma, S.; Kuruppath, S.; Nair, A. V.; Sharma, U., Efflux pumps of Mycobacterium tuberculosis play a significant role in antituberculosis activity of potential drug candidates. *Antimicrob Agents Chemother* **2012,** *56* (5), 2643-51. DOI: 10.1128/AAC.06003-11.

8.   Novak, E.; Schlagel, C. A.; LeZotte, L. A.; Pfeifer, R. T., The tolerance of high dose intravenous spectinomycin therapy in man. *J Clin Pharmacol* **1974,** *14* (8), 442-7.

9.   Hoeksema, H.; Argoudelis, A. D.; Wiley, P. F., Chemistry of Actinospectacin. II. The Structure of Actinospectacin. *Journal of the American Chemical Society* **1962,** *84* (16), 3212-13.

10.   Foley, L.; Lin, J. T.; Weigele, M., Spectinomycin chemistry. III.9-EPI-4(R)-dihydrospectinomycin and 9-epi-spectinomycin. *J Antibiot (Tokyo)* **1978,** *31* (10), 985-90.

11.   Foley, L.; Lin, J. T.; Weigele, M., Spectinomycin chemistry. II.) 9-Deoxy-4(R)-dihydrospectinomycin and 9-deoxyspectinomycin. *J Antibiot (Tokyo)* **1978,** *31* (10), 979-84.

12.   Rosenbrook, W., Jr.; Carney, R. E.; Egan, R. S.; Stanaszek, R. S.; Cirovic, M.; Nishinaga, T.; Mochida, K.; Mori, Y., Spectinomycin modification. IV. 7-deoxy-4(R)-dihydrospectinomycin. *J Antibiot (Tokyo)* **1978,** *31* (5), 451-5.

13.   Thomas, R. C.; Fritzen, E. L., Spectinomycin modification. III. Spectinomycin analogs with C-3'-branched chain sugars. *J Antibiot (Tokyo)* **1985,** *38* (2), 208-19.

14.   White, D. R.; Maring, C. J.; Cain, G. A., Synthesis and in vitro antibacterial properties of alkylspectinomycin analogs. *J Antibiot (Tokyo)* **1983,** *36* (3), 339-42.

15.   Woitun, E.; Maier, R.; Wetzel, B.; Reuter, W.; Lechner, U., Modification of spectinomycin. 2. Derivatives of 4-dihydro-4-deoxy-4(R)-aminospectinomycin. *J Antibiot (Tokyo)* **1981,** *34* (1), 22-7.

16.   Bruhn, D. F.; Waidyarachchi, S. L.; Madhura, D. B.; Shcherbakov, D.; Zheng, Z.; Liu, J.; Abdelrahman, Y. M.; Singh, A. P.; Duscha, S.; Rathi, C.; Lee, R. B.; Belland, R. J.; Meibohm, B.; Rosch, J. W.; Bottger, E. C.; Lee, R. E., Aminomethyl spectinomycins as therapeutics for drug-resistant respiratory tract and sexually transmitted bacterial infections. *Sci Transl Med* **2015,** *7* (288), 288ra75. DOI: 10.1126/scitranslmed.3010572.

17.   Adams, K. N.; Takaki, K.; Connolly, L. E.; Wiedenhoft, H.; Winglee, K.; Humbert, O.; Edelstein, P. H.; Cosma, C. L.; Ramakrishnan, L., Drug tolerance in replicating mycobacteria mediated by a macrophage-induced efflux mechanism. *Cell* **2011,** *145* (1), 39-53. DOI: 10.1016/j.cell.2011.02.022.

18.   Madhura, D. B.; Liu, J.; Meibohm, B.; Lee, R. E., Phase II Metabolic Pathways of Spectinamide Antitubercular Agents: A Comparative Study of the Reactivity of 4-Substituted Pyridines to Glutathione Conjugation. *Medchemcomm* **2016,** *7* (1), 114-117. DOI: 10.1039/C5MD00349K.

19.   Madhura, D. B.; Lee, R.; Meibohm, B., Pharmacokinetic profile of spectinomycin in rats. *Pharmazie* **2013,** *68* (8), 675-676. DOI: 10.1691/ph.2013.3501.

20. Bruhn, D. F.; Scherman, M. S.; Liu, J.; Scherbakov, D.; Meibohm, B.; Bottger, E. C.; Lenaerts, A. J.; Lee, R. E., In vitro and in vivo Evaluation of Synergism between Anti-Tubercular Spectinamides and Non-Classical Tuberculosis Antibiotics. *Sci Rep* **2015,** *5*, 13985. DOI: 10.1038/srep13985.

21. Herrinton, P. M.; Klotz, K. L.; Hartley, W. M., Oxidation and Alkylation of Spectinomycin Derivatives - Synthesis of Trospectomycin from Spectinomycin. *J Org Chem* **1993,** *58* (3), 678-682. DOI: DOI 10.1021/jo00055a021.

22. Friesner, R. A.; Banks, J. L.; Murphy, R. B.; Halgren, T. A.; Klicic, J. J.; Mainz, D. T.; Repasky, M. P.; Knoll, E. H.; Shelley, M.; Perry, J. K.; Shaw, D. E.; Francis, P.; Shenkin, P. S., Glide: a new approach for rapid, accurate docking and scoring. 1. Method and assessment of docking accuracy. *J Med Chem* **2004,** *47* (7), 1739-49. DOI: 10.1021/jm0306430.

23. Case, D. A.; Darden, T. A.; Cheatham, T. E.; Cheatham, I., T.A, AMBER 11. *(University of California, San Francisco, 2010)* **2010**.

24. Wang, J.; Wolf, R. M.; Caldwell, J. W.; Kollman, P. A.; Case, D. A., Development and testing of a general amber force field. *J Comput Chem* **2004,** *25* (9), 1157-74. DOI: 10.1002/jcc.20035.

25. Aqvist, J., Ion Water Interaction Potentials Derived from Free-Energy Perturbation Simulations. *J Phys Chem-Us* **1990,** *94* (21), 8021-8024.

26. Bruell, C. M.; Eichholz, C.; Kubarenko, A.; Post, V.; Katunin, V. I.; Hobbie, S. N.; Rodnina, M. V.; Bottger, E. C., Conservation of bacterial protein synthesis machinery: initiation and elongation in Mycobacterium smegmatis. *Biochemistry* **2008,** *47* (34), 8828-39. DOI: 10.1021/bi800527k.

27. Hurdle, J. G.; Lee, R. B.; Budha, N. R.; Carson, E. I.; Qi, J.; Scherman, M. S.; Cho, S. H.; McNeil, M. R.; Lenaerts, A. J.; Franzblau, S. G.; Meibohm, B.; Lee, R. E., A microbiological assessment of novel nitrofuranylamides as anti-tuberculosis agents. *J Antimicrob Chemother* **2008,** *62* (5), 1037-45. DOI: 10.1093/jac/dkn307.

28. Rakesh; Bruhn, D.; Madhura, D. B.; Maddox, M.; Lee, R. B.; Trivedi, A.; Yang, L.; Scherman, M. S.; Gilliland, J. C.; Gruppo, V.; McNeil, M. R.; Lenaerts, A. J.; Meibohm, B.; Lee, R. E., Antitubercular nitrofuran isoxazolines with improved pharmacokinetic properties. *Bioorg Med Chem* **2012,** *20* (20), 6063-72. DOI: S0968-0896(12)00645-1 [pii] 10.1016/j.bmc.2012.08.023.

29. North, E. J.; Scherman, M. S.; Bruhn, D. F.; Scarborough, J. S.; Maddox, M. M.; Jones, V.; Grzegorzewicz, A.; Yang, L.; Hess, T.; Morisseau, C.; Jackson, M.; McNeil, M. R.; Lee, R. E., Design, synthesis and anti-tuberculosis activity of 1-adamantyl-3-heteroaryl ureas with improved in vitro pharmacokinetic properties. *Bioorg Med Chem* **2013,** *21* (9), 2587-99. DOI: 10.1016/j.bmc.2013.02.028.

30. Lenaerts, A. J. M.; Gruppo, V.; Brooks, J. V.; Orme, I. M., Rapid in vivo screening of experimental drugs for tuberculosis using gamma interferon gene-disrupted mice. *Antimicrob Agents Ch* **2003,** *47* (2), 783-785. DOI: 10.1128/Aac.47.2.783-785.2003.

For Table of Contents Use Only

The Structure-Activity Relationships of Spectinamide Antituberculosis agents; a Dissection

of Ribosomal Inhibition and Native Efflux Avoidance Contributions

Jiuyu Liu,[1] David F. Bruhn,[1] Robin. B. Lee,[1] Zhong Zheng,[1] Tanja Janusic,[2] Dimitri

Scherbakov,[2] Michael S. Scherman,[3] Helena I. Boshoff,[4] Sourav Das,[1] Rakesh,[1] Samanthi L.

Waidyarachchi,[1] Tiffany A. Brewer, [1, 5] Begoña Gracia,[6] Lei Yang,[1] John Bollinger,[1] Gregory T.

Robertson,[3] Bernd Meibohm,[5] Anne J. Lenaerts,[3] Jose Ainsa,[6] Erik C. Böttger,[2] Richard E. Lee[1*]

Graphical Abstract